



Performance of Alkali Activated Slag Stabilized Landfill Mined Soil-Like Fraction Exposed to Different Climatic Conditions

A. Sandeep Reddy¹ · Kannan K. R Iyer¹ · Veerabhadra M. Rotte¹ · Trudeep N. Dave¹

Received: 12 June 2024 / Accepted: 30 August 2024
© The Author(s), under exclusive licence to Springer Nature Switzerland AG 2024

Abstract

Landfill mined soil-like fraction (LMSF) is the material obtained from mining of old waste. Utilization of LMSF in infrastructure applications is limited due to several challenges including possible presence of organic content, heavy metals, heterogeneous composition, etc., and require stabilization prior to usage. In light of this, LMSF was stabilized with alkali activated slag at different curing temperatures including freeze curing (-21°C), ambient curing (25°C), thermal curing (60°C) and their combinations. Further, the performance of stabilized LMSF was evaluated on cyclic exposure to different climatic conditions, viz., -21°C , 0°C , 10°C , 25°C and 45°C in both closed (without water exposure) and open system (water inundated) conditions. The performance of stabilized LMSF under these climatic conditions was evaluated through unconfined compressive strength (UCS), indirect tensile strength, cyclic loading tests, and microstructural aspects. Based on initial trials, ambient curing (25°C) and 2 days thermal curing at 60°C yielded better performance of stabilized LMSF. The 28 days stabilized LMSF has shown stable performance against cyclic exposure to different climatic conditions by satisfying the maximum allowable mass loss criteria after 12 cycles as per IRC-37, except for exposure to subfreezing temperature of -21°C in open system. Further, not much reduction in UCS and indirect tensile (except for -21°C in open system) strength was observed on cyclic exposure to different climatic conditions, inferring the stability of cementitious compounds and resistance against degradation. 2 days of thermal curing at 60°C notably enhanced the performance of stabilized LMSF in different exposure conditions under both static and cyclic loading conditions, suggesting it as favourable curing condition for sustainable and low-cost stabilization of LMSF in different climatic conditions ranging from sub-freezing to arid regions.

Keywords Freezing and thawing · Thermal curing · Climatic conditions · Alkali activated slag · Landfill waste · Durability

Introduction

Landfill mined soil-like fraction (LMSF) is the soil-like material obtained from mining of the old legacy waste. Unlike combustibles and construction debris, LMSF has very limited applications, such as filling up of low-lying

areas, utilization as daily landfill cover material, or re-landfilling [1]. The utilization of LMSF as a material or energy source is restricted due to its heterogeneity in material composition, presence of organic matter, variability in engineering properties, leachability of heavy metals, low calorific values, and high ash content [2]. Song et al. [3] found that increase in organic content led to decrease in shear strength upon utilizing solid waste from landfills in road construction. Further, the decomposition of organic matter may lead to higher settlement, formation of cavities and affects the overall performance of infrastructure facilities. The presence of heavy metals (when exceeds the permissible limits) in LMSF may cause subsurface and ground water contamination with the possible percolation of leachate under heavy rainfall or flooding events.

Suitable pre-treatment methods such as soil washing, soil vitrification, and bioremediation can be employed to overcome the challenges associated with presence of

✉ Veerabhadra M. Rotte
vmrotte@iitram.ac.in

A. Sandeep Reddy
annapureddy.reddy.21pc@iitram.ac.in

Kannan K. R Iyer
kannaniyer@iitram.ac.in

Trudeep N. Dave
trudeepdave@iitram.ac.in

¹ Department of Civil Engineering, Institute of Infrastructure, Technology, Research and Management, Ahmedabad 380026, India

organic matter or heavy metals in LMSF. In addition to pre-treatment methods, adopting suitable stabilization/reinforcement techniques can be beneficial for improving the engineering performance of LMSF, and to satisfy the specifications for target infrastructure applications. Recent studies explored the utilization of fibre reinforcement to improve the engineering behaviour of LMSF for subgrade fill, embankment fill, and backfilling applications [4, 5]. Studies have shown that reinforcing LMSF fills with geosynthetic materials can enhance the bearing capacity up to 1.8 times in comparison to untreated LMSF [6]. Rawat and Mohanty [7] demonstrated the enhanced behaviour of LMSF reinforced with geosynthetics under static loading conditions. Ram et al. [8] investigated the utilization of LMSF, along with fly ash and locally available soils, as layered systems under foundations as a fill material. However, the utilization of LMSF aiming towards pavement infrastructure (as subgrade, subbase, and base course) is still unexplored. Further, the stabilization of LMSF through alkali activation of sustainable binders like ground granulated blast furnace slag (GGBS) and fly ash, is also less explored, and the performance of stabilized LMSF under various climatic conditions remains to be understood.

Alkali activated binders are primarily composed of pozzolanic materials like GGBS, fly ash, silica fume, and alkali compounds such as NaOH, KOH, and Na_2SiO_3 . The alkaline compounds particularly support in the activation of inert aluminosilicate compounds present in pozzolanic materials. Many researchers in the past evaluated the efficiency of alkali activated stabilization for different soils ranging from silty sands to soft clays [9, 10]. Assessing both mechanical properties and durability characteristics are crucial in evaluating the effectiveness of alkali activated binders in stabilizing soils/geomaterials. Moreover, the performance of soils/geomaterials stabilized through alkali activation depends on different factors such as curing time, curing temperature, binder content, activator content, exposure to different climatic conditions, type of soil/geomaterial, etc. [11].

The exposure to different climatic conditions plays a vital role in overall performance of the soils/geomaterials stabilized through alkali activation. In particular, the regions with subfreezing temperature requires more attention as the long-term stability and durability characteristics of stabilized soils/geomaterials may get severely affected due to cyclic freezing and thawing action [12, 13]. The pore water present in the soil/geomaterial voids gets frozen at subfreezing temperature and increases its volume by approximately 9% [14], resulting in the development of internal tensile stresses in the soil/geomaterial pore spaces. This phenomenon will ultimately lead to the development of micro- and macro-cracks at different levels, and these cracks propagate further and may lead to instability and collapse of the structure [15,

16]. Thus, the stability of the cementitious compounds will greatly affect the overall performance of the stabilized soils/geomaterials.

Many researchers in the past reported superior performance of soils stabilized through alkali activation under different climatic conditions ranging from subfreezing conditions to arid conditions [17, 18]. Aryal et al. [19] studied the long-term durability of stabilized kaolin soil; wherein, a cement content of 10% and 0.5% polypropylene fibres were optimised based on the wetting-drying and freezing-thawing studies. Fakhrabadi et al. [20] utilised copper slag and NaOH as alkaline activator to stabilize clayey sand soils, and reported an optimum copper slag content and NaOH concentration of 15% and 8M, respectively. Jamalimoghadam and Bahmyari [21] studied the effect of alkaline activated binder in stabilizing marl clays against freezing and thawing cycles and concluded that the parameters including concentration of alkaline activator, binder content and number of freezing-thawing cycles governs the overall efficiency of the stabilized soils. Samantasinghar and Singh [22] evaluated the mechanical and durability characteristics of sandy soils stabilized with sodium hydroxide (NaOH) activated fly ash and GGBS. An increased compressive strength was noticed in stabilized soils on exposure to wetting-drying and freezing-thawing cycles due to the continuous geopolymerisation and hydration actions during these phases. Though, alkali activated stabilization was well studied for natural soils, there is a need to explore the performance of alkali activated stabilization of LMSF, under different climatic conditions, ranging from sub-freezing to arid regions, for its potential utilization as an alternate material. In this context, the authors have investigated the effect of alkali activated stabilization of LMSF on its strength and durability properties under different climatic conditions. The durability characteristics were evaluated through cyclic exposure to various climatic conditions. The details of materials utilized, experimental methodology adopted, as well as results and discussion from the study are presented in the following sections.

Materials

Landfill Mined Soil-Like Fraction (LMSF)

The landfill mined soil-like fraction (LMSF) utilized in the present study was obtained from a landfill site located in Ahmedabad, India. LMSF was obtained from the landfill site after screening of the landfill mined waste through a trommel screener that removes the construction debris, recyclables, and combustibles. The LMSF obtained from the landfill site was further pre-processed in laboratory (air drying followed by mechanical sieving through 4.75 mm sieve) to obtain the fraction that was free from any traces of

undesired matter (viz., fibres/floating material, wood residue, small cloth pieces, oversize fraction greater than 4.75 mm, etc.) and was utilized for further analysis.

Figure 1a represents the typical particle size distribution curve obtained for LMSF, and is classified as SP-SM (Poorly graded sand with silt) according to ASTM D2487 [23]. The liquid limit of LMSF was observed in the range of 35.3–36.2%, and is non-plastic in nature as per ASTM D4318 [24]. The LMSF utilized in the current study contains an organic content in the range of 1.40–2.68% evaluated accordance to ASTM D2974 [25]. Specific gravity was obtained as per ASTM D854 [26] for LMSF as fibres/floating material was not observed in the study, and the values were in the range of 2.28–2.41. An average maximum dry density of 16.2 kN/m³ with an average optimum water content of 18.5% was obtained through standard Proctor test conducted as per ASTM D698 [27]. Unconfined compression strength (UCS) tests on LMSF specimens performed as per the recommendations of ASTM D2166 [28], yielded an average UCS value of about 80 kPa. Inductively Coupled Plasma (ICP) analysis was conducted on leachate extracted from LMSF to assess the presence of heavy metals as per ASTM D3987 [29]. The average concentration of heavy metals (average

of three samples) present in the LMSF was assessed and were found to be within the permissible limits outlined by USEPA and Flemish regulatory standards [30, 31], as depicted in the Fig. 1b. Hence, no pre-treatment of LMSF was envisaged in the present study.

The XRD spectra of LMSF (Fig. 1c) reveals the presence of quartz and calcite peaks confirming the existence of silica and lime compounds. Additionally, the presence of microcline and albite indicates the existence of sodium-based minerals. Similar inferences were drawn from FTIR spectra of LMSF sample (Fig. 1d), wherein, the peaks around a wavelength of 500 cm⁻¹ indicate the presence of O–Si–O bonds (quartz), while peaks of C–H and C–O suggest traces of organic compounds in LMSF [32, 33], wherein the peaks of O–H denote the presence of residual moisture in LMSF [34]. The presence of calcite (CaCO₃) was further confirmed from Thermogravimetric analysis (TGA) as depicted in the Fig. 1e, with peaks around 650–700 °C indicating the potential presence of calcium carbonate/calcite mineral and the peak related to evaporation of residual water was noticed around 50–100 °C [35]. Further, Fig. 1f presents the SEM (scanning electron microscopy) image of LMSF, revealing agglomeration of fine particles observed alongside the coarser grains, and finer fractions of LMSF adhering to the surface of coarser grains.

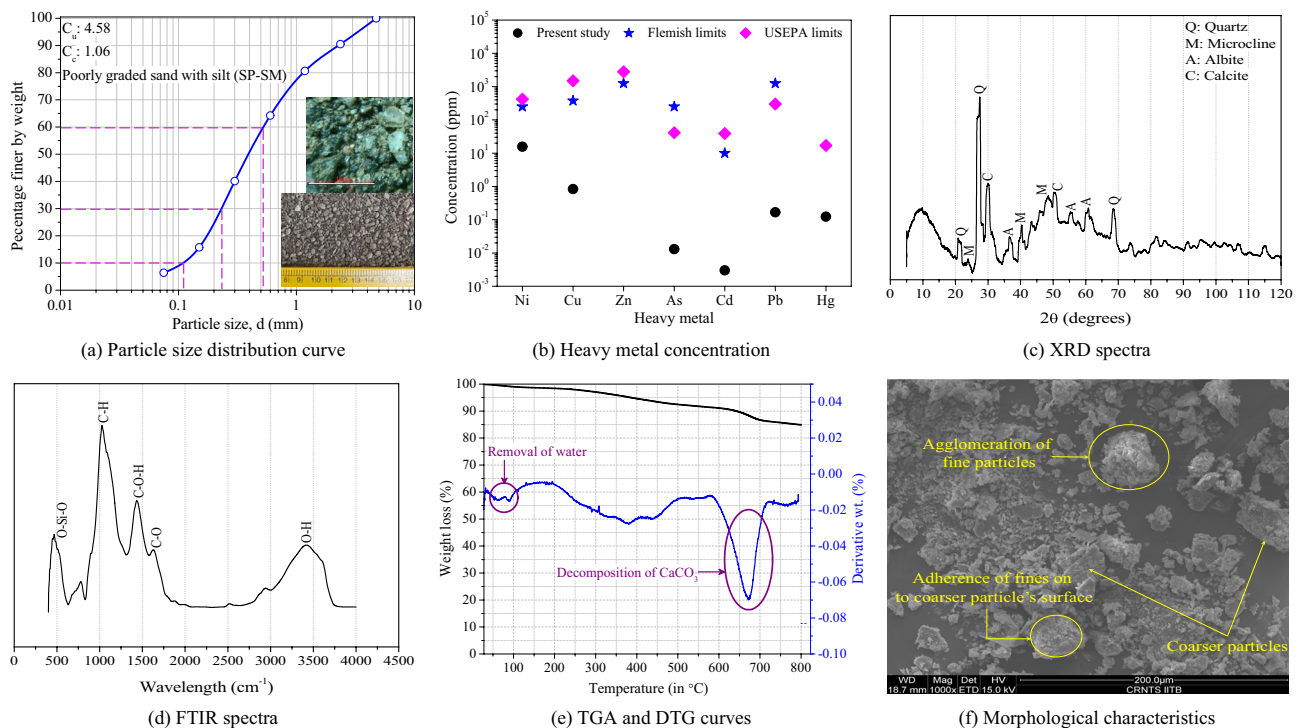


Fig. 1 Particle size distribution, heavy metal concentration and microstructural (XRD, FTIR, TGA and SEM) characteristics of LMSF

Ground Granulated Blast Furnace Slag (GGBS) and Alkaline Activators

Ground granulated blast furnace slag (GGBS), is an industrial by-product from iron and steel manufacturing industries, and was procured commercially to serve as a pozzolanic material in the study. GGBS primarily comprises of amorphous silica and calcium, and readily gets activated by alkaline activators to produce free silicate and aluminate ions [36]. The GGBS utilized in the study consists of 37.42% SiO₂, 26.20% CaO, 15.50% Fe₂O₃, 13.52% Al₂O₃, and other minor compounds. Laser diffraction study reveals an average particle size of approximately 6.47 μm for GGBS. The specific gravity and specific surface area of GGBS were obtained as 2.97 and 277.04 m²/kg, respectively.

A composite alkaline activator consisting of sodium hydroxide (NaOH) and sodium silicate (Na₂SiO₃) was employed in the present study to activate GGBS. An industrial grade NaOH flakes were commercially procured, and an alkaline NaOH solution (3% of dry weight of LMSF that corresponds to 4.2 M concentration as detailed in methodology section) was prepared by dissolving NaOH pellets in distilled water. NaOH being highly alkaline, rapidly elevates the mixture's pH, facilitating the dissolution of amorphous silica and aluminium compounds. On the other hand, Na₂SiO₃ (M_s = 1.03; where, M_s is silica modulus) was also commercially procured and composed of 28.30% Na₂O, 29.24% SiO₂ and 42.46% H₂O. Na₂SiO₃ primarily facilitates the development of nucleation sites, aiding the availability of silicate ions and contributes to the development of hydration products.

Methodology

The testing program in this study was divided into three main phases. In the first phase, the GGBS and activator content were optimised based on unconfined compressive strength test (UCS). The second phase focuses on selecting the appropriate curing condition, including curing temperature and curing age. Finally, in the third phase, the performance of stabilized LMSF on cyclic exposure to different climatic conditions, was evaluated through mass loss, UCS and split tensile strength. Cylindrical specimens of size 38 mm × 76 mm prepared at a dry density of 16.2 kN/m³ and optimum moisture content of 18.5% were utilized for the evaluation of UCS and split tensile strength as per the guidelines of ASTM D2166 [28] and ASTM C496 [37], respectively. A displacement rate of 1.25 mm/min was adopted in the current study and four specimens were tested for each combination, and the average of four specimens, along with the range of variation, is presented in the study. Further, cyclic UCS tests were performed on selected combinations

at peak loads of 0.8P and 0.7P (P is the UCS for the combination), to assess the behaviour of stabilized LMSF under cyclic loading conditions. The microstructural features were also studied for selected combinations through FTIR and optical imaging studies.

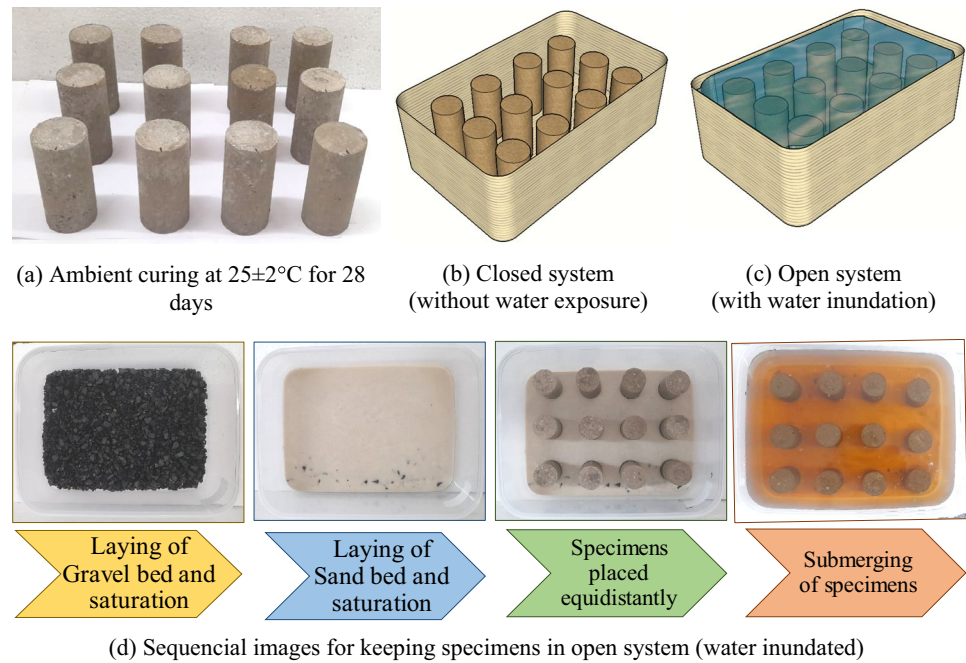
Optimisation of Binder, Activator and Curing Conditions

In first phase, a total binder (GGBS and NaOH + Na₂SiO₃) replacement percentage ranging from 10 to 40% was investigated, along with varying percentages of activators (NaOH + Na₂SiO₃) from 2 to 8%. Optimization was achieved by evaluating the UCS values of the trial combinations at a curing period of 7 days. In the second phase, the effective curing regime was identified by evaluating 7 days UCS strength of optimised combination under different curing temperature and time. Five different curing regimes were considered including (a) 7 days of curing at 25 °C, (b) 2 days of curing at 60 °C followed by 5 days at 25 °C, (c) 2 days of curing at 60 °C followed by 5 days at – 21 °C, (d) 2 days of curing at 25 °C followed by 5 days at – 21 °C, and (e) 7 days of curing at – 21 °C. These curing regimes were evaluated to determine the most economic and suitable curing condition for LMSF stabilization through alkali activated slag, with focus on moderate as well as sub-freezing climatic conditions.

Performance Assessment under Different Climatic Conditions

The performance of stabilized LMSF (in terms of strength and durability), was evaluated by exposing the specimens to different climatic conditions. The specimens were initially cured at an ambient temperature of 25 ± 2 °C for 28 days as shown in Fig. 2a, and were subsequently exposed to cycles of different climatic conditions prior to performance assessment. Five different climatic exposure conditions were considered in the present study, including – 21 °C and 0 °C (sub-freezing and freezing conditions), 10 °C (cold region), 25 °C (moderate climate), and 45 °C (arid region), representing a wide range of climatic conditions prevailing across the world. At the onset, the specimens of optimised combinations were subjected to their respective temperature regime (– 21 °C, 0 °C, 10 °C, 25 °C, or 45 °C) for 24 h. Following this period, they were extracted from respective temperature conditions and were allowed to undergo thawing, warming, or cooling at 25 °C for next 24 h, which completes one cycle of freezing-thawing/cooling-warming/heating-cooling. Subsequently, the specimen surfaces were scraped with a wire brush to remove any disintegrated particles, following recommendations of ASTM D560 [38], and their mass was recorded after each cycle. The above procedure was repeated for 12 cycles and the residual

Fig. 2 Methodology adopted for exposure of specimens to different climatic conditions



strength after 12 cycles of exposure was evaluated in terms of UCS and split tensile strength.

Two distinct conditions including closed system and open system as shown in Fig. 2b, c, respectively, were considered during exposure to different climatic conditions as suggested by Wong and Haug [39]. In closed system, no additional water supply was permitted apart from the water present in soil/geomaterial voids during exposure to different climatic conditions [40, 41]. This system typically reflects field conditions, where there is minimal or no change in the in-situ moisture content during different times of the year [42]. In contrast, an open system refers to the free movement of pore water in soil/geomaterial voids during exposure to different climatic conditions. In an open system, a non-uniform distribution of ice lenses is anticipated, reflecting seasonal variations in the in-situ moisture content for soil/geomaterial [39]. Permeable soils, such as gravels and sands, are more susceptible to open system conditions, while fine-grained soils tend to exhibit closed system behaviour due to their low permeability. In the present study, for open system, a bottom bed comprising of gravel (1 cm thick) overlain by sand (1 cm thick) was provided along with a water head of 2 cm above top surface of the specimen as represented in Fig. 2d. The summary of different climatic exposure conditions utilized in present study is presented in Table 1.

Results and Discussion

Optimisation of Binder and Activator Content

To optimize the GGBS and activator content (including NaOH:Na₂SiO₃ ratio), unconfined compression strength (UCS) tests were conducted on 7 days cured specimens, and the results are depicted in Fig. 3. The optimization was mainly carried out in three stages, wherein in initial stage the binder content was varied in the range of 10–40%, with GGBS content ranging from 4 to 34%, while maintaining a constant activator content of 6% (3% NaOH + 3% Na₂SiO₃). In second stage, activator content was varied in the range of 2–8% at the optimised binder content, and finally the ratio of NaOH:Na₂SiO₃ was varied from 1:1 to 1:2.5, at the optimised binder and activator content. An UCS strength of 2000 kPa (as per AUSTRROADS [43]) was selected as the target strength for 28 days of curing, and the combinations achieving 70% of the target strength within 7 days of curing were selected as optimised combination for further evaluation.

As illustrated in Fig. 3a, a non-linear increase in UCS strength is noticed with the increase of binder content from

Table 1 Various curing and exposure climatic conditions adopted in the current study

Combination	Curing conditions	Post-curing exposure regime		NaOH:Na ₂ SiO ₃
		Exposure temperature	Exposure condition	
C1 _(7D)	7 days at 25 °C	(No exposure)		1:1
C2 _(7D)	2 days at 60 °C and 5 days at 25 °C	(No exposure)		1:1
C3 _(7D)	2 days at 60 °C and 5 days at – 21 °C	(No exposure)		1:1
C4 _(7D)	2 days at 25 °C and 5 days at – 21 °C	(No exposure)		1:1
C5 _(7D)	7 days at – 21 °C	(No exposure)		1:1
C6 _(28D) CS _(– 21 °C)	28 days at 25 °C	– 21 °C (F) and 25 °C (T)	Closed system	1:1
C7 _(28D) CS _(0 °C)	28 days at 25 °C	0 °C (F) and 25 °C (T)		1:1
C8 _(28D) CS _(10 °C)	28 days at 25 °C	10 °C (C) and 25 °C (W)		1:1
C9 _(28D) CS _(25 °C)	28 days at 25 °C	25 °C (A) and 25 °C (A)		1:1
C10 _(28D) CS _(45 °C)	28 days at 25 °C	45 °C (H) and 25 °C (C)		1:1
C6 _(28D) OS _(– 21 °C)	28 days at 25 °C	– 21 °C (F) and 25 °C (T)	Open system	1:1
C7 _(28D) OS _(0 °C)	28 days at 25 °C	0 °C (F) and 25 °C (T)		1:1
C8 _(28D) OS _(10 °C)	28 days at 25 °C	10 °C (C) and 25 °C (W)		1:1
C9 _(28D) OS _(25 °C)	28 days at 25 °C	25 °C (A) and 25 °C (A)		1:1
C10 _(28D) OS _(45 °C)	28 days at 25 °C	45 °C (H) and 25 °C (C)		1:1
C11 _(56D)	56 days at 25 °C	(No exposure)		1:1
C12 _(56D)	56 days at 25 °C	(No exposure)		1:2.5
C13 _(28D) CS _(– 21 °C)	28 days at 25 °C	– 21 °C (F) and 25 °C (T)	Closed system	1:2.5
C14 _(56D)	2 days at 60 °C, 53 days at – 21 °C & 01 day rest at 25 °C	(No exposure)		1:1
C15 _(28D) CS _(– 21 °C)	2 days at 60 °C and 26 days at – 21 °C	– 21 °C (F) and 25 °C (T)	Closed system	1:1

A, Ambient; C, Cooling; CS, Closed system (without water inundation); D, Days; F, Freezing; H, Heating; NaOH, sodium hydroxide; Na₂SiO₃, sodium silicate; OS, Open system (with water inundation); T, Thawing; W, Warming

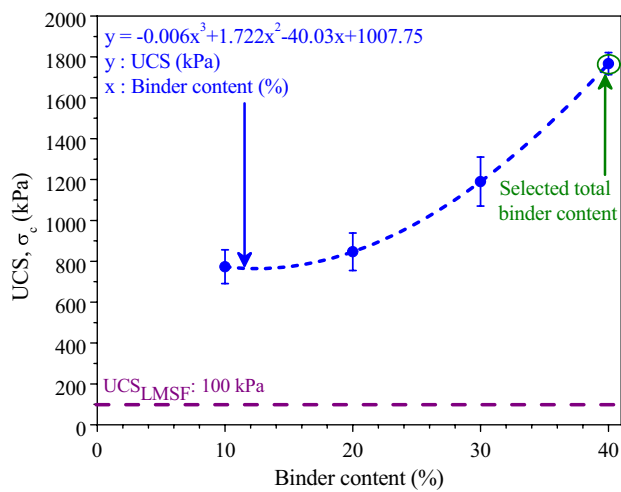
0 to 40%, and a binder content of about 40% has yielded a 7 days UCS strength of 1765 kPa and was selected as optimum binder content in the study. Further, at 40% binder replacement content, the activator percentage was varied from 2 to 8%, and a non-linear increase in 7 days UCS values is observed with increase of activator content as shown in Fig. 3b. However, owing to the target UCS criterion and minimal activator usage (from sustainability and economical perspectives), an activator content of 6% has been considered suitable in the current study. Further, a linearly decreasing trend of UCS was observed with a reduction in NaOH:Na₂SiO₃ ratio (viz., increase in proportion of Na₂SiO₃) as shown in Fig. 3c, as the increase of silicate ions leads to an increase in setting time and alters the hydration reactions.

However, all the activator ratios satisfied the target UCS criterion, and among all the activator ratios 1:1 has yielded better efficiency with a UCS value of 1765 kPa at 7 days curing. Hence, the combination of 60% LMSF, 34% GGBS, 3% NaOH, and 3% Na₂SiO₃ was selected for further studies. Additionally, as increasing Na₂SiO₃ in activator combination was considered more sustainable, the combination of 60% LMSF, 34% GGBS, 1.7% NaOH, and 4.3% Na₂SiO₃ (with

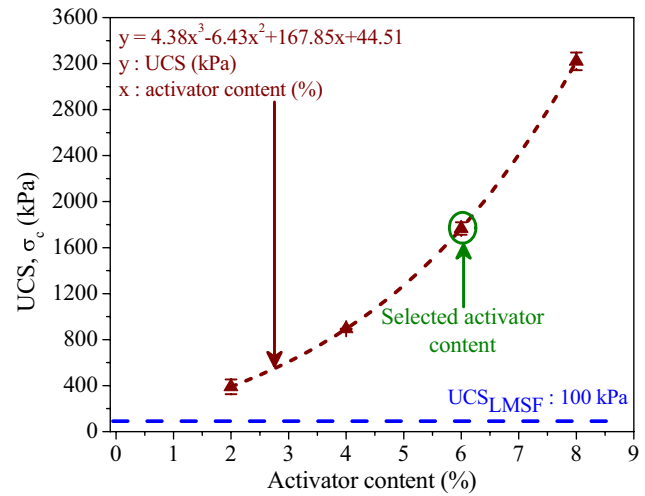
a NaOH to Na₂SiO₃ ratio of 1:2.5) was also considered for durability assessment and compared with the standard combination (with NaOH:Na₂SiO₃ as 1:1).

Optimisation of Curing Regime

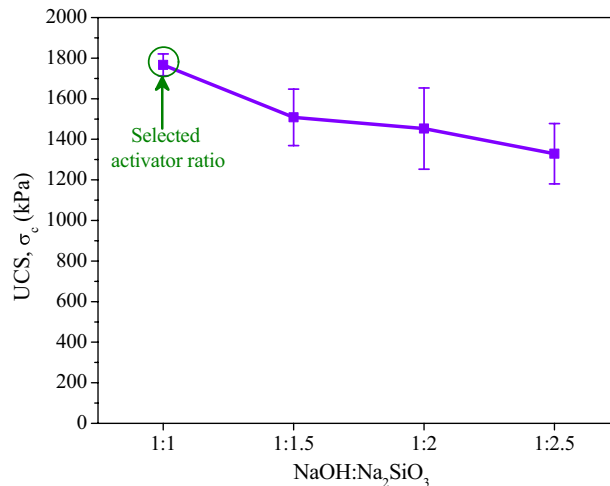
Figure 4a, b illustrate the typical stress-strain response and UCS results of 7 days cured specimens under various curing regimes. It can be observed from Fig. 4 that the average UCS values of around 2368 kPa and 2900 kPa are obtained for specimens subjected to 2 days of thermal curing at 60 °C followed by 5 days of ambient curing (25 °C) and 5 days of freeze curing (– 21 °C), respectively, as compared to an average UCS value of 1765 kPa for 7 days of ambient curing (25 °C). Further, not much effect on the UCS values was observed on curing at – 21 °C after an initial curing at 60 °C and 25 °C for 2 days, inferring the stability of developed cementitious compounds during initial curing phases. Figure 4c represents the FTIR spectra obtained for the combinations thermally cured for 2 days at 60 °C, and 2 days of thermal curing at 60 °C followed 5 days of freeze curing (– 21 °C). The peaks identified around 1000 cm^{–1} and 500 cm^{–1} represent the presence of Si–O and Si–O–Si



(a) 7 days UCS values with varying binder content (at constant NaOH + Na₂SiO₃ = 6%)



(b) Variation of activator content (NaOH + Na₂SiO₃) in 40% binder replacement



(c) Variation of NaOH:Na₂SiO₃ ratio in 6% activator content

Fig. 3 Optimisation of GGBS and activator content

bonds respectively, indicate the formation of cementitious compounds such as CSH/CASH/NASH [44]. The carbonate peaks identified around 900 cm⁻¹ and 1450 cm⁻¹ represents the presence of CaCO₃ and/or Na₂CO₃ [45]. The presence of pore water was confirmed from the peaks of H–O–H observed around 1650 cm⁻¹ and 3500 cm⁻¹ [34]. Thus, the cementitious compounds developed under initial 2 days thermal curing at 60 °C can be considered to be stable on further curing at – 21 °C.

Conventionally, during ambient curing, the free residual water present in the soil/geomaterial matrix dissolves in the activator solution and dilutes the activator, leading to decreased alkalinity in the soil/geomaterial matrix [46]. However, with initial thermal curing, the residual water

evaporates, reducing the dilution of activator, which in turn increases alkalinity levels in the soil/geomaterial matrix and hence results in higher UCS values due to better reactivity at higher pH. The increase in pH levels promotes hydration reactions at a much faster rate and accounts for the subsequent development of cementitious compounds [47]. A much lower UCS values were observed for specimens subjected to 2 days ambient curing (25 °C) followed by 5 days of freeze curing (– 21 °C), and for those subjected to 7 days of freeze curing (– 21 °C), possibly due to inhibition of poly-condensation reactions [48]. Based on these results, 7 days ambient curing (25 °C) was selected as standard curing condition in the present study owing to its potential utilization during summer in cold regions, for curing in moderate

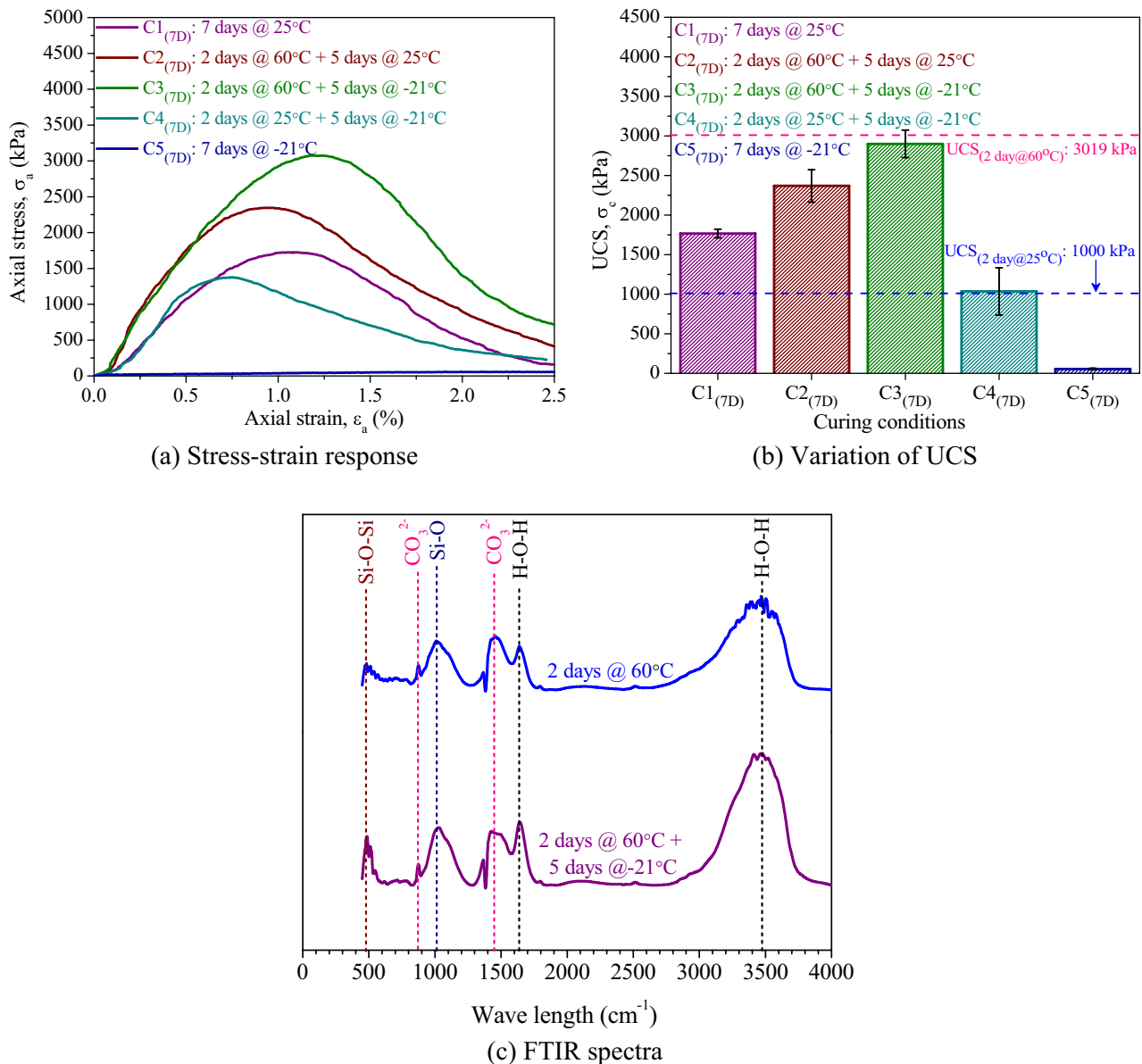


Fig. 4 Stress–strain response, UCS and FTIR spectra for stabilized LMSF under different curing regimes

climatic conditions, and during winter in arid climatic conditions. Further, the performance of ambient cured specimens was compared with 2 days of thermal curing (60 °C) followed by 5 days freeze curing (− 21 °C) condition, keeping in view the need for cold regions during winter.

Mechanical Assessment of Stabilized LMSF Cured at Ambient Conditions (25 °C)

Figure 5 shows the typical mechanical assessment results obtained for stabilized LMSF cured at ambient conditions (25 °C). Specimens cured for different durations exhibited a relatively brittle failure with negligible post-peak

strength after failure, as illustrated by the stress-strain characteristics in Fig. 5a. From Fig. 5b, it can be noted that almost 70% of the 28 days UCS strength was achieved within 3 days of curing, indicating a rapid rate of hydration reactions during early age. The rapid development of CSH / CASH gels during alkali activated stabilization in the initial curing period can be mainly attributed due to the development of high pH levels in soil/geomaterial system [49, 50]. However, as curing time progresses, the pH in the geomaterial (viz., soil/LMSF) matrix decreases, and the development of alkali aluminosilicate gels (geo-polymerisation) becomes dominant. Consequently, a decline in the rate of strength gain can be observed after 3 days of

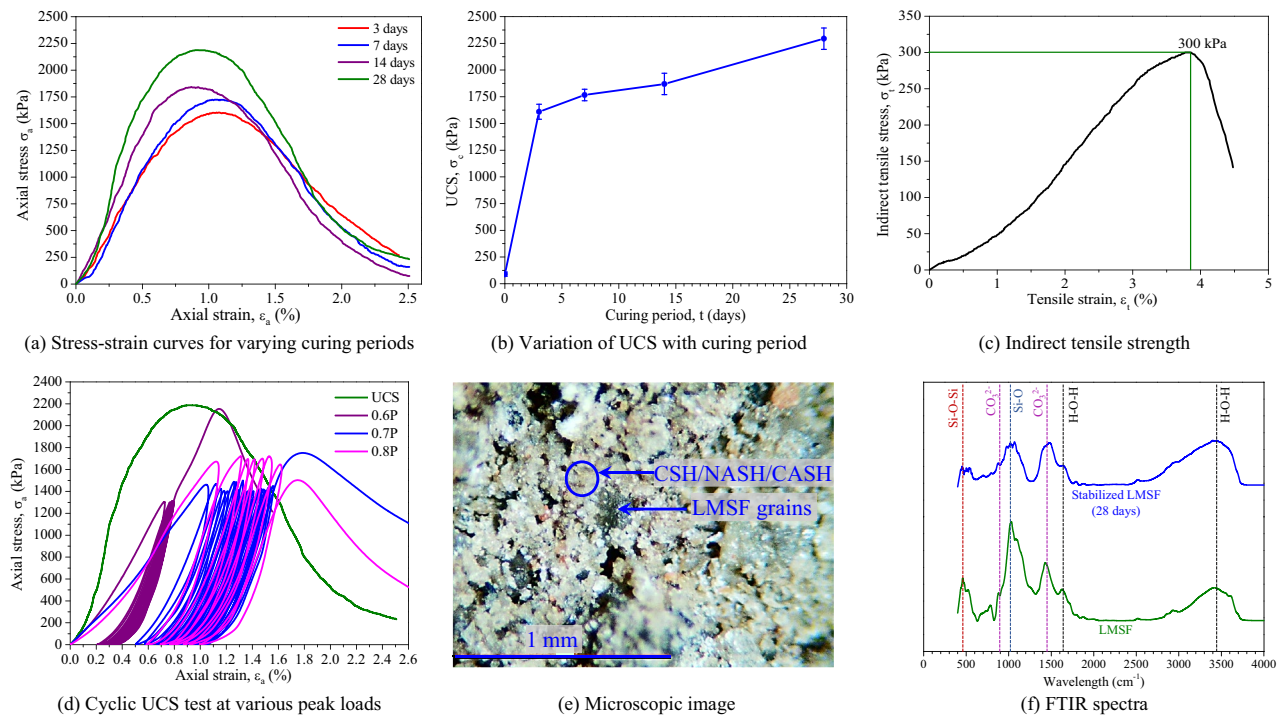


Fig. 5 Mechanical and microstructural assessment of 28 days alkali activated stabilization of LMSF at 25 °C

curing. An average UCS strength of about 2240 kPa was achieved within 28 days of curing satisfying the desired criterion of 2000 kPa for subbase/base course applications as per AUSTROADS [43]. Further, an average split tensile strength of about 300 kPa was noted for stabilized LMSF with 28 days of curing as shown in Fig. 5c.

The typical response to 25 cycles of cyclic loading at 0.6P, 0.7P, and 0.8P loading (where P is the average failure load from UCS tests) is presented in Fig. 5d. A reduction of about 15% and 30% in the peak stress in comparison to UCS value was observed at 0.7P and 0.8P loading conditions. The decrease in the peak stress can be mainly attributed due to the fatigue effects induced by cyclic loading. However, no reduction in peak stress was noticed at 0.6P loading condition, suggesting the negligible fatigue effects under this loading condition. Further, Fig. 5e represents the optical image of stabilized LMSF, and a well distributed cementitious matrix, binding the LMSF grains can be observed from the optical image. Fig. 5f shows the FTIR spectra for unstabilized LMSF and stabilized LMSF after 28 days curing. The presence of Si–O–Si peak around 450 cm^{-1} in LMSF refers to the presence of quartz minerals, while the Si–O–Si peak in stabilized LMSF refers to the existence of cementitious compounds such as CSH/NASH/CASH [44]. The presence of carbonate peaks in stabilized LMSF around wavelengths of 900 cm^{-1} and 1450 cm^{-1} , suggest the possible precipitation of calcite or sodium carbonate through

hydration reactions [45]. Peaks around 1620 cm^{-1} and 3420 cm^{-1} can be attributed to the presence of water [34].

Performance on Exposure to Various Climatic Conditions after Ambient Curing

The UCS specimens of stabilized LMSF combination (60% LMSF + 34% GGBS + 3% NaOH + 3% Na_2SiO_3) were subjected to ambient curing at a temperature of 25 °C for 28 days as discussed above and were subsequently exposed to 12 cycles of different climatic conditions (2 days per cycle \times 12 cycles = 24 days) followed by 4 days of rest period in ambient conditions, as presented in Table 1. Thus, the specimens were tested after 56 days (28 days ambient curing + 24 days exposure to different climatic conditions + 4 days of rest period) after casting. The results obtained in terms of cumulative mass loss, stress-strain response, UCS, indirect tensile strength, and microstructural aspects (FTIR and optical imaging) are discussed in the subsequent sections.

Evaluation of the Cumulative Mass Loss

Figure 6a, b depict the cumulative percentage mass loss observed during cyclic exposure to various climatic conditions under closed system and open system conditions, respectively. An average cumulative mass loss percentage of about 1.88%, 1.51%, 1.23%, 1.05%, and 1.11%, were

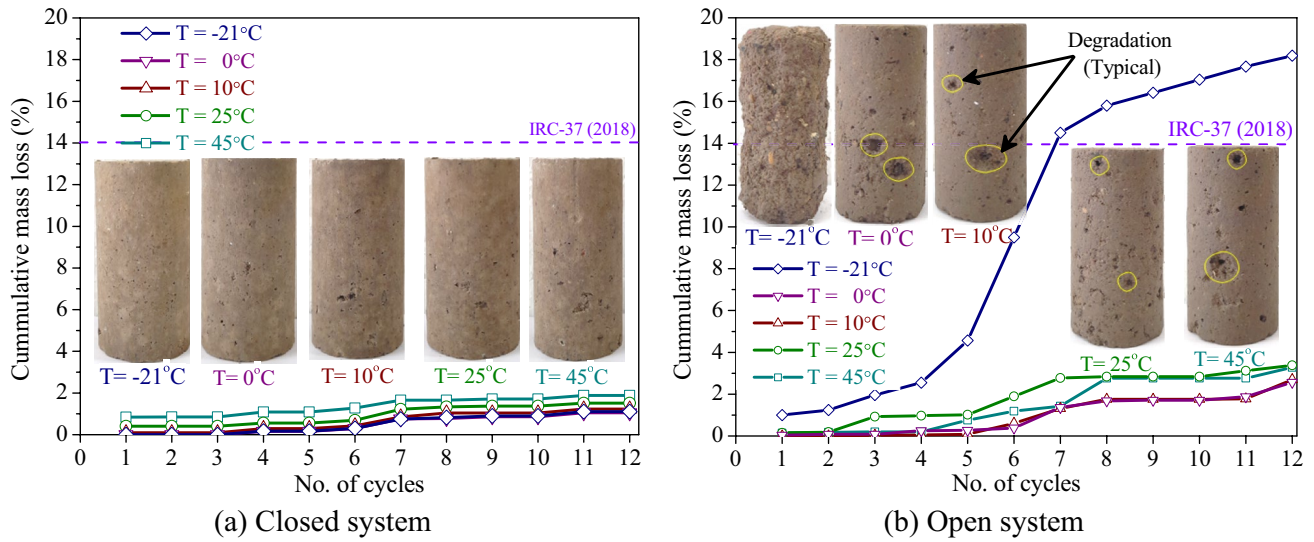


Fig. 6 Variation of cumulative mass loss on cyclic exposure to different climatic conditions

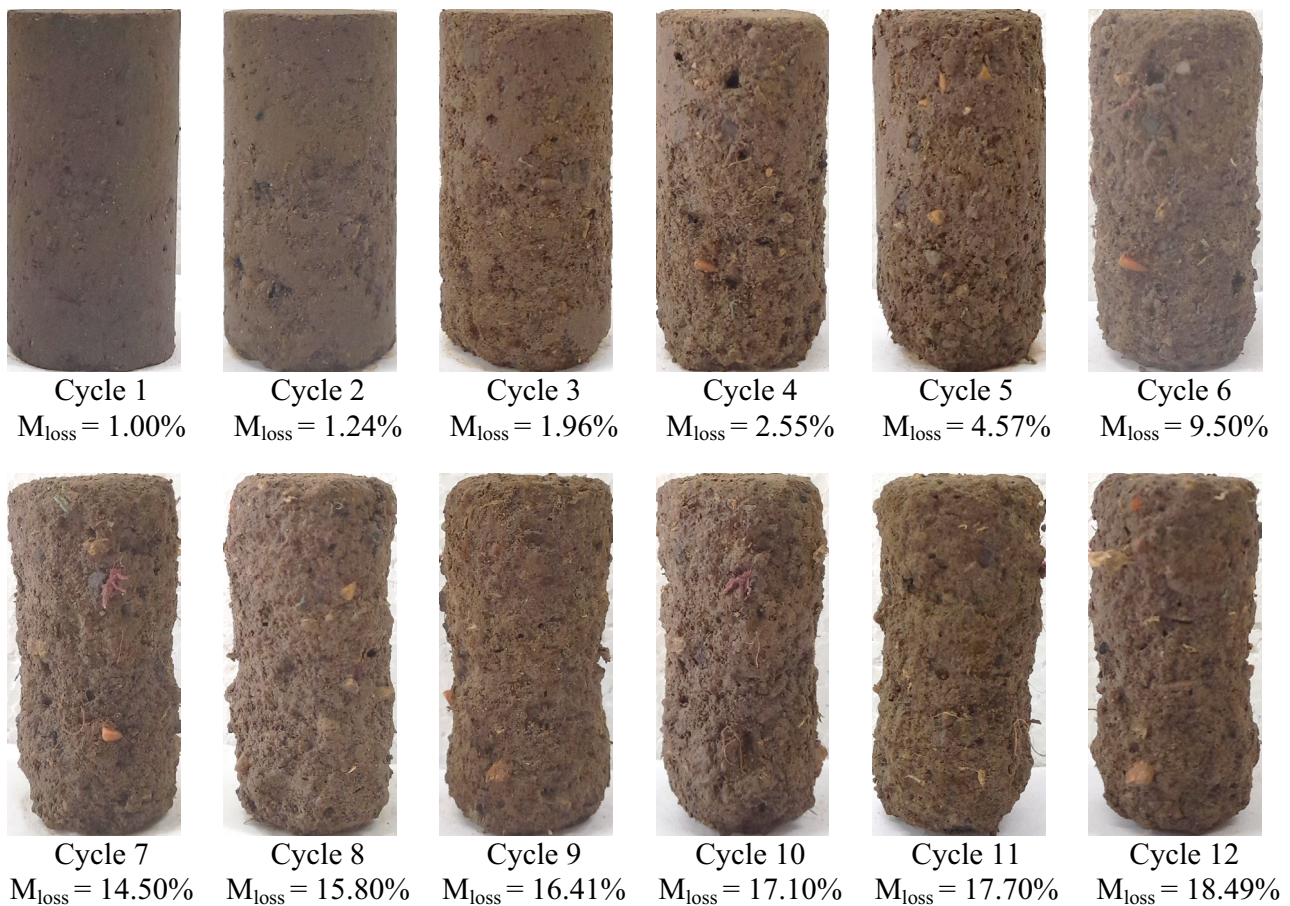


Fig. 7 Cumulative percentage mass loss of specimens after exposure to cycles of freezing (– 21 °C) and thawing (25 °C) cycles in open system

noted after 12 cycles of exposure in closed system conditions, for specimens exposed to 45 °C, 25 °C, 10 °C, 0 °C, and – 21 °C, respectively and subsequent thawing/cooling/warming at ambient temperature. Similarly, in open system conditions, an average cumulative mass loss percentage of about 3.28%, 3.38%, 2.70%, 2.57%, and 18.49% were noted after 12 cycles of exposure to 45 °C, 25 °C, 10 °C, 0 °C, and – 21 °C, and subsequent thawing/cooling/warming at ambient temperature. A maximum mass loss of about 18.49% (progressive degradation with typical images is shown Fig. 7) was observed after 12 cycles of freeze-thaw exposure at – 21 °C and 25 °C in open system condition. The higher degradation of LMSF mass in open system was mainly attributed to the prolonged immersion of specimens in water. In open system, the specimens experienced the combined effects of ambient wetting and freezing/cooling/heating due to which erosion from stabilized LMSF surface was observed, while no surface erosion was noticed in closed system. Further, with the possible movement of water in LMSF pore spaces in open system, a higher spalling of LMSF mass was noticed that may lead to the development of minor and macro cracks in stabilized LMSF matrix. A much similar phenomenon was observed by Altun et al. [14] on exposure to freeze and thaw of stabilized silty soils. In summary, the stabilized LMSF under both closed and open systems satisfied the permissible percentage mass loss criteria of 14% as specified by IRC-37 [51], except for the subfreezing temperature exposure condition of – 21 °C under open conditions. The variation of pH and EC for specimens exposed to open system was monitored to understand the reasons for degradation in more details under different climatic exposure conditions, and are discussed in the following section.

Variation of pH and EC in Open System

Figure 8a depicts the variation of pH with number of exposure cycles for specimens exposed to open system conditions. Initially, a pH in the range of 10–10.5 was observed, indicating the likely leaching of hydroxyl ions (OH⁻) from the stabilized LMSF matrix to the surrounding water, during the first exposure cycle. The high leaching rate during initial exposure cycles was associated with the dissolution of unreacted activator and GGBS compounds. However, with increase in the exposure cycles, pH values were noted to reduce linearly and a stable pH of around 9.5 was achieved after 8 cycles of exposure. This suggests that the dissolution of unreacted activators and GGBS reached a plateau and indicates the cessation or near cessation of leaching. Similarly, Fig. 8b illustrates the variation of electrical conductivity (EC) with number of exposure cycles for specimens exposed in open system. An initial EC of around 7–12.8 mS/cm was noted for different exposure conditions, and a linear reduction in EC values were observed with increase in the number of exposure cycles. Similar to pH, a constant EC of around 0.8 mS/cm was attained after 8 cycles of exposure. Similar findings were reported by Aldaood et al. [12] on lime-stabilized gypseous soils, wherein, reduced EC values were primarily attributed to gypsum dissolution.

Stress-Strain Behaviour and Compressive Strength Characteristics

Figure 9a, b show the average stress-strain curves obtained from UCS tests after exposure to different climatic conditions, in closed system and open system, respectively. Figure 9a represents a typical brittle nature

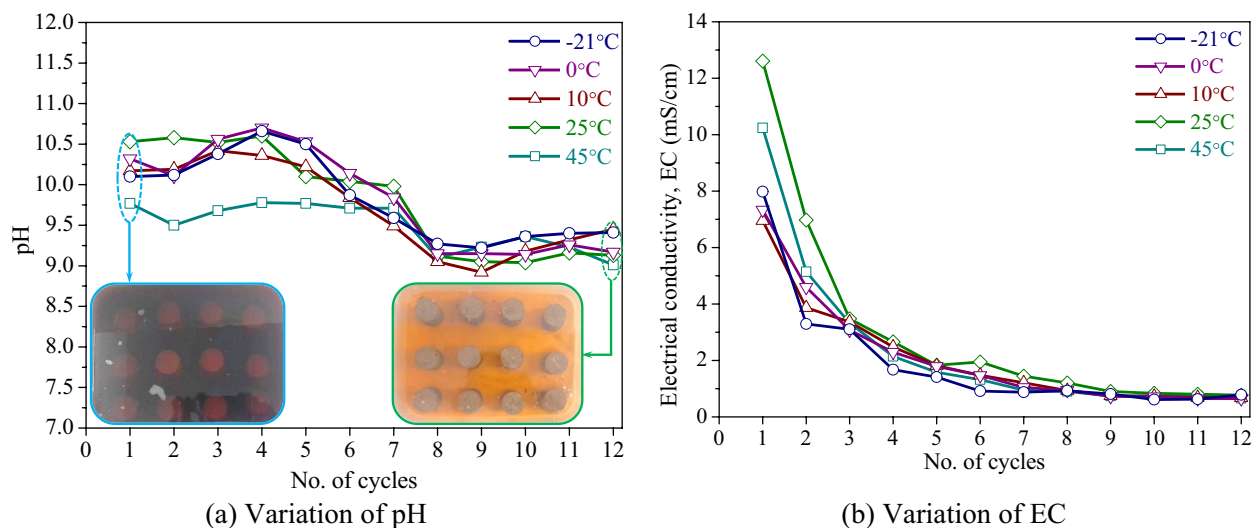
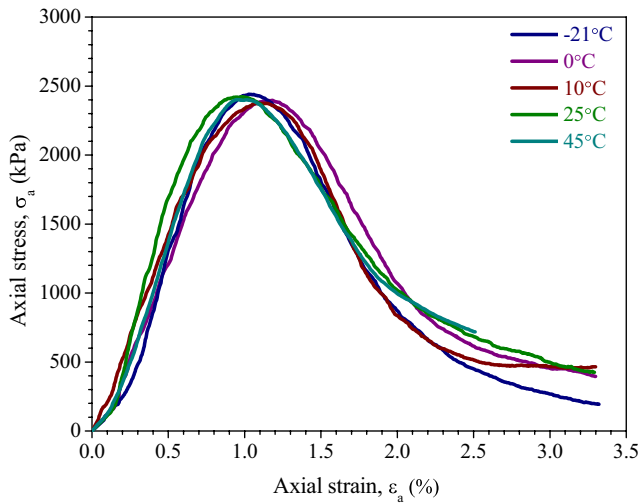
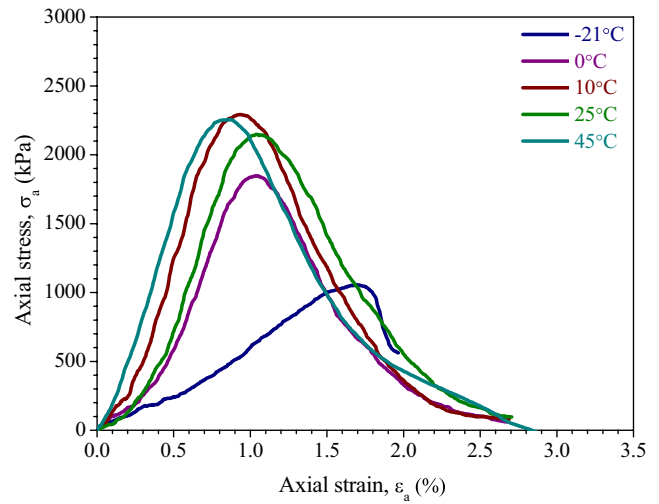


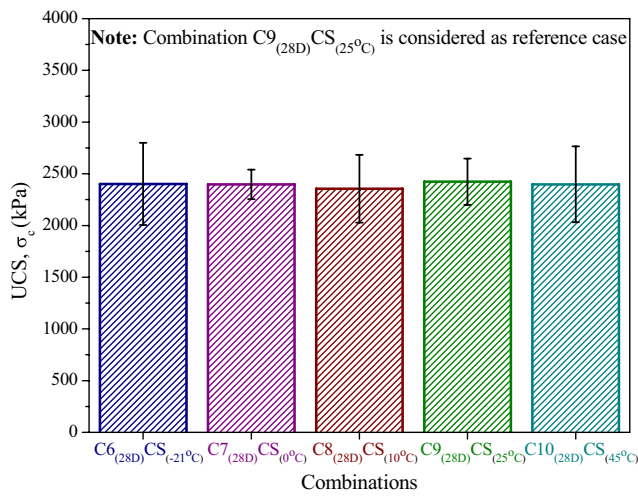
Fig. 8 Variation of pH and electrical conductivity (EC) on exposure to different climatic conditions



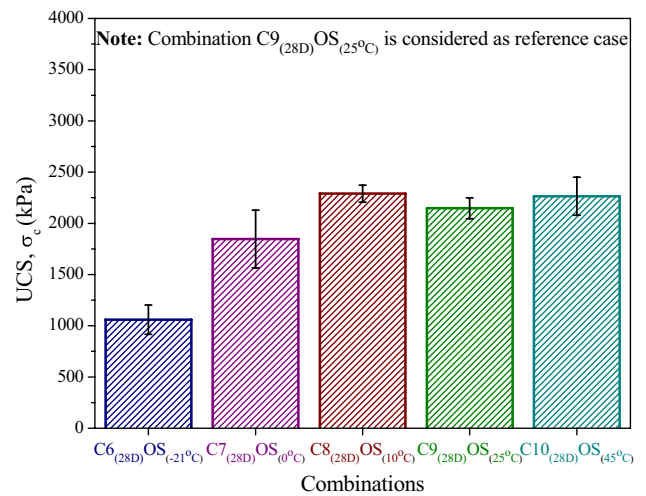
(a) Stress-strain response (closed system)



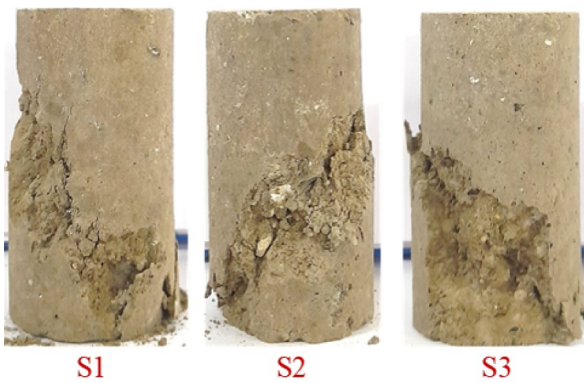
(b) Stress-strain response (open system)



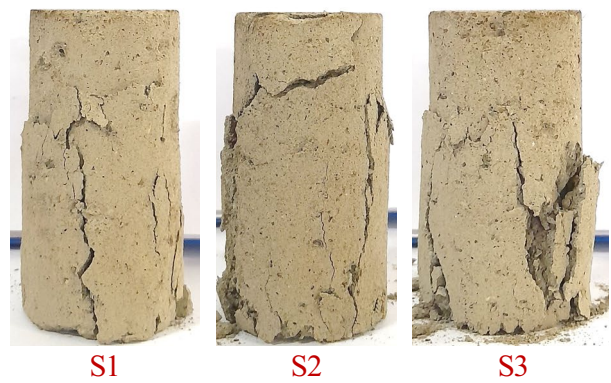
(c) UCS (closed system)



(d) UCS (open system)



(e) Typical failure images (closed system)



(f) Typical failure images (open system)

Fig. 9 Stress–strain response, UCS and typical failure images on exposure to different climatic conditions

with peak stress at around 1.2% strain, followed by a post peak reduction in stress with negligible residual strength in closed system condition. Similar behaviour is observed from Fig. 9b in open system conditions, wherein, a slightly lower peak strain of around 0.9 to 1% is noticed, except for $-21\text{ }^{\circ}\text{C}$ exposure condition where significantly lower peak stress and higher corresponding strain are observed, probably due to rapid degradation (viz., disintegration and mass loss) causing reduction in strength and higher deformation, under subfreezing conditions.

Figure 9c, d represent the average UCS values along with the range (represented by error bars) obtained for different specimens of a combination under closed and open system, respectively. An UCS of about 2400 kPa was noted and no degradation in UCS was observed upon cyclic exposure to various climatic conditions in closed system. Similarly, an UCS of around 2150–2290 kPa was noted in open system condition for exposure conditions of $10\text{ }^{\circ}\text{C}$, $25\text{ }^{\circ}\text{C}$ and $45\text{ }^{\circ}\text{C}$. A reduction in the UCS of about 25% and 60% were noted for the exposure conditions of $0\text{ }^{\circ}\text{C}$ and $-21\text{ }^{\circ}\text{C}$ (freezing/sub-freezing temperatures), respectively. The reduction of UCS in freezing/sub-freezing temperatures in open system was mainly attributed due to the combined effects of saturation of specimens due to wetting and freezing of pore water in the stabilized LMSF voids that caused volume expansion. The volume expansion is expected to result in the development of internal tensile stresses in the pore space and initiate the development of micro cracks in LMSF pore structure [14, 15, 52]. With more exposure cycles, water retention in pores increases, possibly widening the micro cracks into macro cracks that contributed to reduce the UCS values at $0\text{ }^{\circ}\text{C}$ and $-21\text{ }^{\circ}\text{C}$. In contrast, no reduction in UCS was observed in closed system, as saturation of the LMSF pores was restricted. Further, the majority of the water contained in the LMSF pores was expected to have already participated in the hydration reactions and converted into stable hydrates. These hydrates were stable under cyclic exposure to different climatic conditions and low amount of residual free water was expected to remain in the LMSF pores. Hence, tensile stresses were not expected to develop on exposure to freezing conditions, resulting in stable structure. These phenomena were further evident from the typical failure images of UCS specimens in closed and open systems (Fig. 9e, f). Specimens in the closed system exhibited shear failure, suggesting uniform stress distribution across the cross-section. Conversely, specimens in the open system exhibited peripheral failure, indicating variation in strength between the inner core and peripheral portion, suggesting the deterioration of peripheral portion on exposure to different climatic conditions.

Tensile Stress–Strain Behaviour and Tensile Strength Characteristics

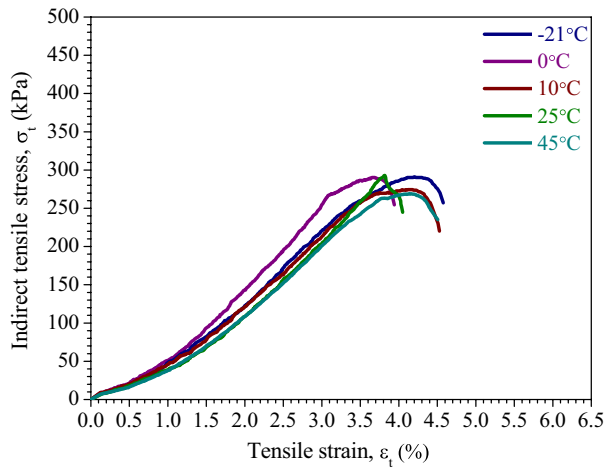
Figure 10a, b represent the tensile stress-strain behaviour of stabilized LMSF specimens on exposure to different climatic conditions. An average peak tensile stress of about 270–300 kPa for different combinations, and a corresponding strain ranging from 3.5 to 4% was observed in closed system; while, average peak tensile stress varying between 325 and 380 kPa for different combinations, with corresponding strain of around 4.5–5%, were noted in open system.

Further, Fig. 10c, d show the variation of indirect tensile strength in closed and open systems, respectively, on exposure to different climatic conditions. An increase in indirect tensile strength of about 16–25% was noted in open system in comparison to closed system, except for $-21\text{ }^{\circ}\text{C}$, wherein, a higher degradation of specimen was noted. The increase of tensile strength in open system could be possibly attributed to better cementation in the inner core of specimens with the availability of extra water and prolonged cementation leading to the increased stiffness of the specimen [53]. Figure 10e, f represent the typical failure images and confirms that all specimens failed by near-perfect split failure, indicating the participation of overall cross-section in the failure.

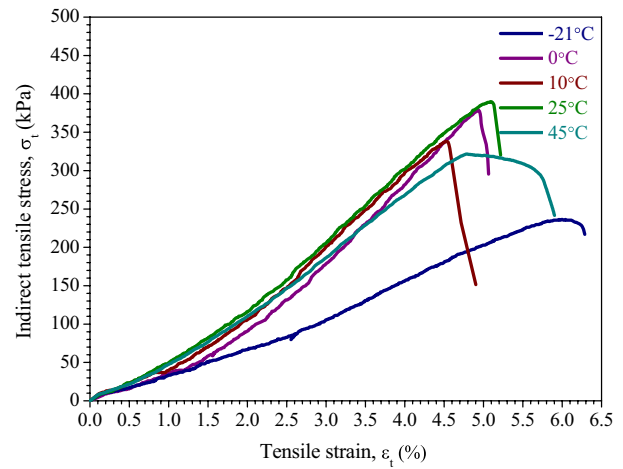
Microstructural Assessment

Figure 11a, b show the FTIR spectra obtained for stabilized LMSF specimens after exposure to different climatic conditions in closed system and open system, respectively. A common peak around 490 cm^{-1} and 1000 cm^{-1} was noticed in all cases, indicating the presence of Si–O–Si and Si–O bonds, suggesting the presence of cementitious compounds such as NASH/CSH/CASH [49]. Additionally, peaks of CO_3^{2-} can be observed around 850 cm^{-1} and 1450 cm^{-1} , indicating possible precipitation of calcite or sodium carbonate in stabilized LMSF matrix [50]. A slightly higher intensity peaks of calcite were noticed in open system inferring the precipitation of higher amount of calcite due to prolonged hydration reactions with availability of additional water during inundation. Presence of H–O–H bonds was also noted in both closed and open system conditions representing the presence of residual or adsorbed water [34]. Overall, the cementitious compounds appear to be stable on cyclic exposure to different climatic conditions in both closed and open systems.

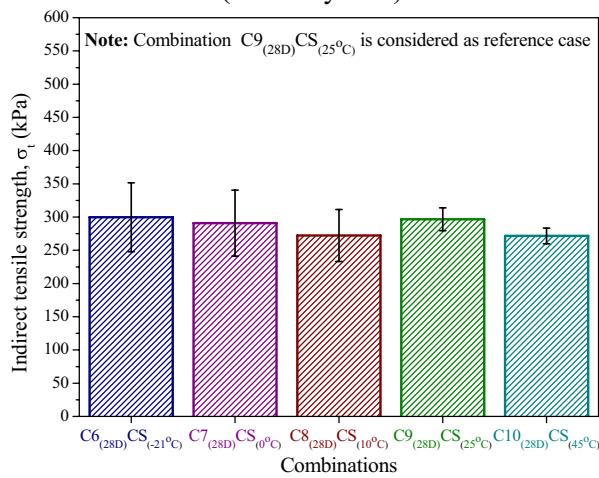
Figure 12 depicts the optical microscopic images of specimens exposed to $25\text{ }^{\circ}\text{C}$, $0\text{ }^{\circ}\text{C}$ and $-21\text{ }^{\circ}\text{C}$ in closed and open systems. A dense cemented LMSF matrix was observed for ambient cured ($25\text{ }^{\circ}\text{C}$) specimens in the closed system (Fig. 12a). However, a slight degradation was noticed in open system due to potential erosion of unreacted slag/LMSF particles, resulting in the development of minor cavities (Fig. 12d). Minor cracks were



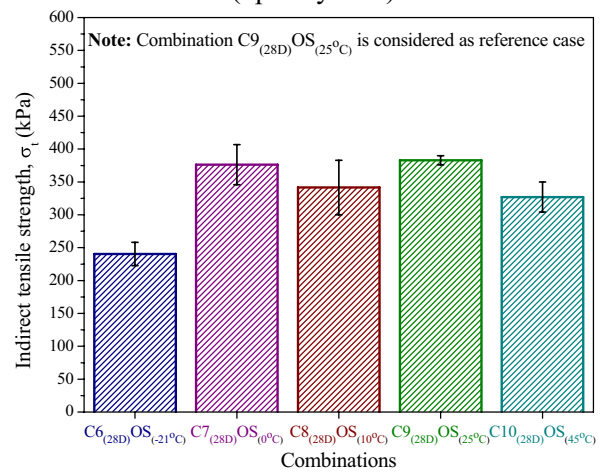
(a) Indirect tensile stress-strain response (closed system)



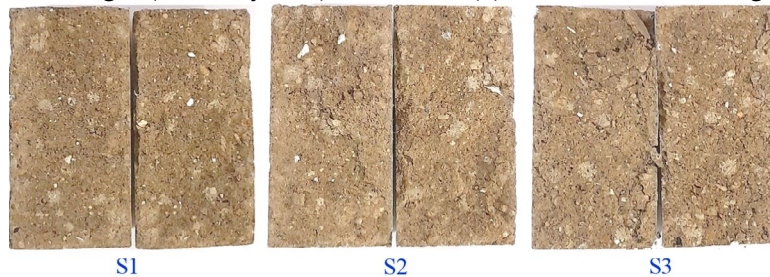
(b) Indirect tensile stress-strain response (open system)



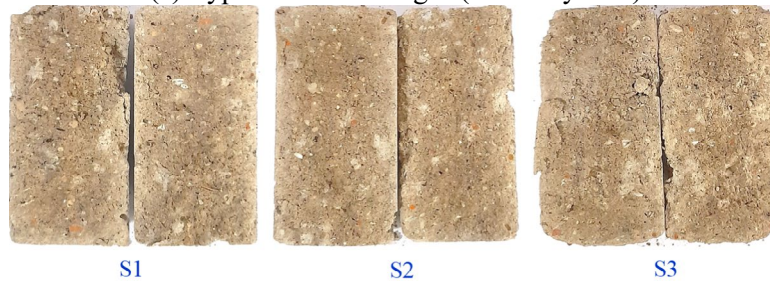
(c) Indirect tensile strength (closed system)



(d) Indirect tensile strength (open system)



(e) Typical failure images (closed system)



(f) Typical failure images (open system)

Fig. 10 Indirect tensile stress-strain response, indirect tensile strength and typical failure images on exposure to different climatic conditions

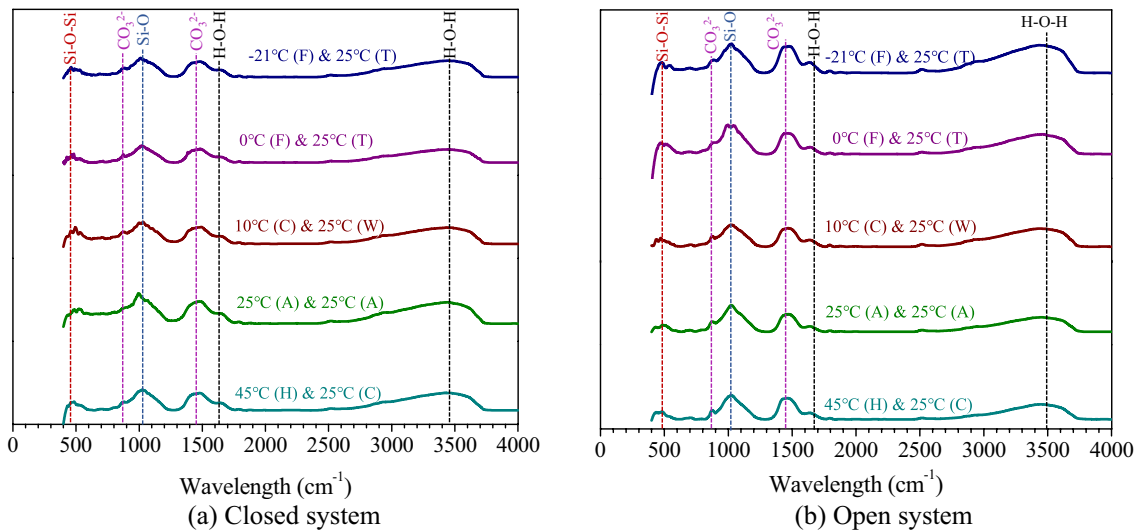


Fig. 11 FTIR spectra of specimens exposed to different climatic conditions

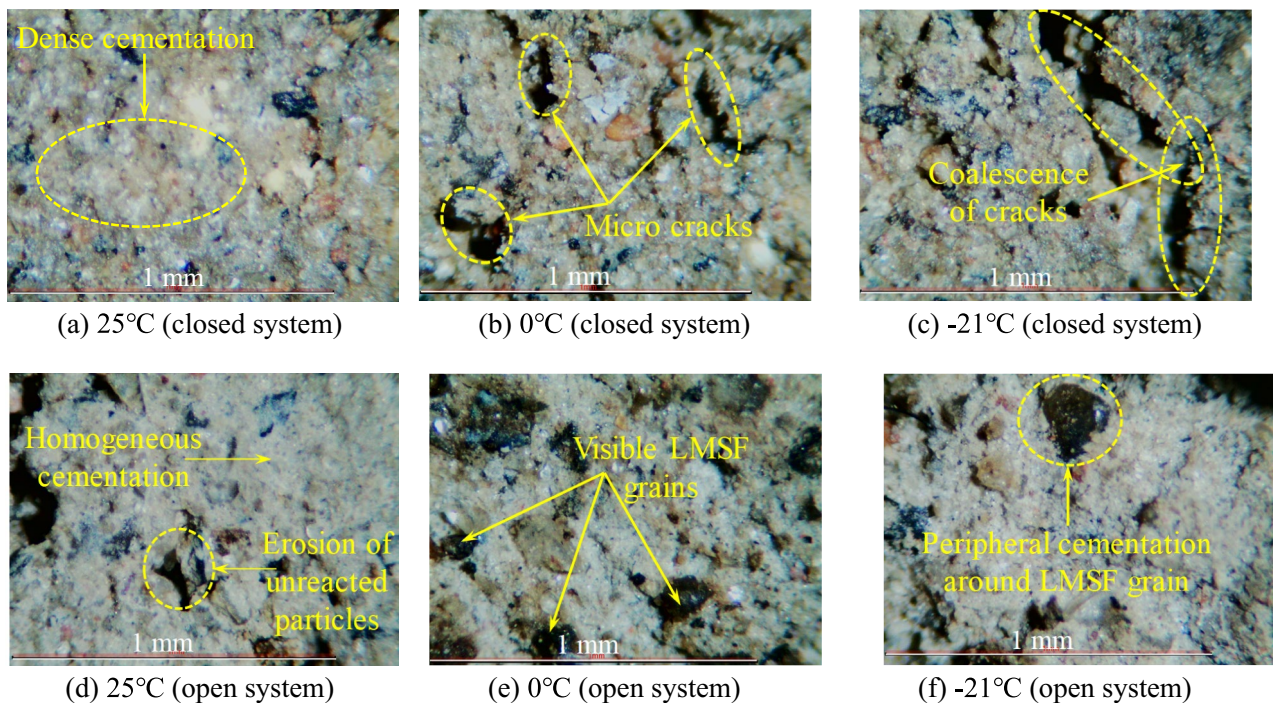


Fig. 12 Optical images (typical) of specimens exposed to 25 °C, 0 °C and – 21 °C

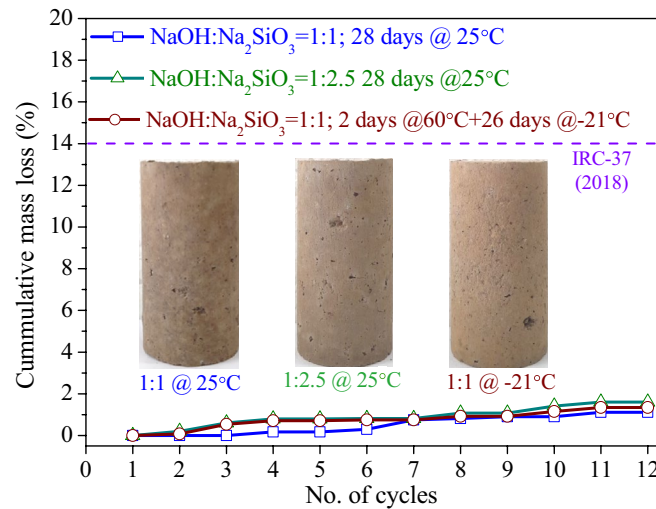
observed in the specimens exposed to 0 °C and – 21 °C in closed system (Fig. 12b, c, respectively) due to freezing of free water into ice lenses (that causes volume expansion). Additionally, localized crack coalescence was also noticed (Fig. 12c) for the specimens exposed at – 21 °C in closed system. On the other hand, specimens that were exposed to 0 °C and – 21 °C in the open system (Fig. 12e, f, respectively) exhibited the combined effects of erosion

and micro cracks attributed to the saturation due to wetting accompanied by expansion due to freezing. Visible LMSF grains indicate the extent of erosion due to wetting, while homogeneous cementation was also noticed, possibly due to leaching of activator solution into the LMSF pores, and prolonged hydration reactions with the availability of water.

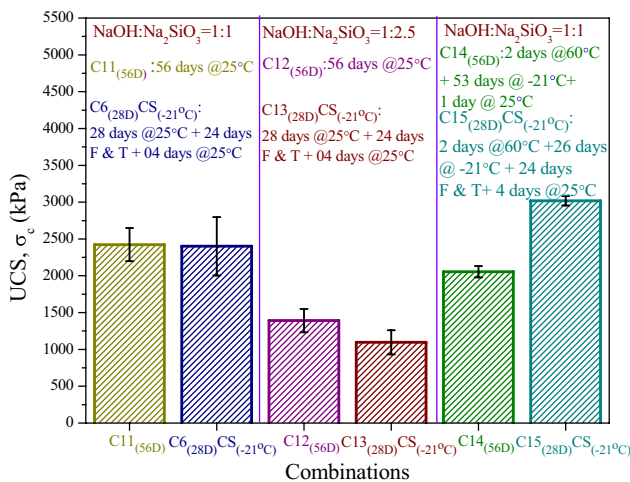
Effect of Thermal Curing (60 °C) and Activator Ratio on Performance of Stabilized LMSF

A comparative assessment was carried out for specimens cured at ambient curing (25 °C) for 28 days and specimens cured at thermal curing (60 °C) for 2 days followed by curing at - 21 °C for the remaining 26 days. Further, the effect of NaOH:Na₂SiO₃ as 1:2.5 (low proportion of NaOH) was also compared with NaOH:Na₂SiO₃ as 1:1 (high proportion of NaOH). Lowering the amount of NaOH is more sustainable and economical and controls the shrinkage and efflorescence of overall system [54]. The specimens of above combinations were exposed to 12 cycles of freezing (- 21 °C) and thawing (25 °C) in closed system conditions, and their UCS and indirect tensile strength were evaluated and are discussed below.

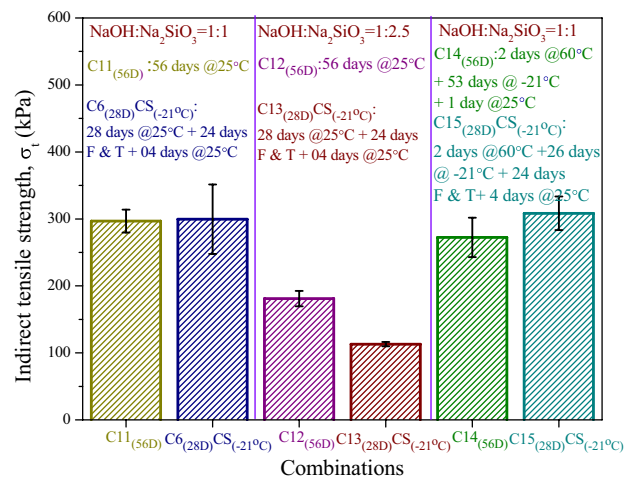
An increase in the mass loss from 1.11 to 1.34% is noted with the increase of NaOH:Na₂SiO₃ ratio from 1:1 to 1:2.5 as shown in Fig. 13a. Further, thermal cured specimens exhibited a mass loss of about 1.30% on 12 exposure cycles in comparison to 1.11% for ambient curing (Fig. 13a). All the combinations have satisfied the criteria of restricting the mass loss to 14% as per IRC-37 [51]. Figure 13b, c represent the variation of UCS and indirect tensile strength for ambient cured specimens (activator ratio of 1:1 and 1:2.5) with and without exposure to freeze-thaw cycles and tested at age of 56 days. The figures also depict the results for specimens cured for 2 days at 60 °C, followed by curing at - 21 °C for 53 days, followed by one day of rest period (activator ratio of 1:1). A decrease in the UCS and indirect tensile strength of about 42.60% and 38.90%, respectively were observed with the increase of NaOH:Na₂SiO₃ ratio from 1:1 to 1:2.5.



(a) Variation of cumulative mass loss



(b) Variation of UCS



(c) Variation of indirect tensile strength

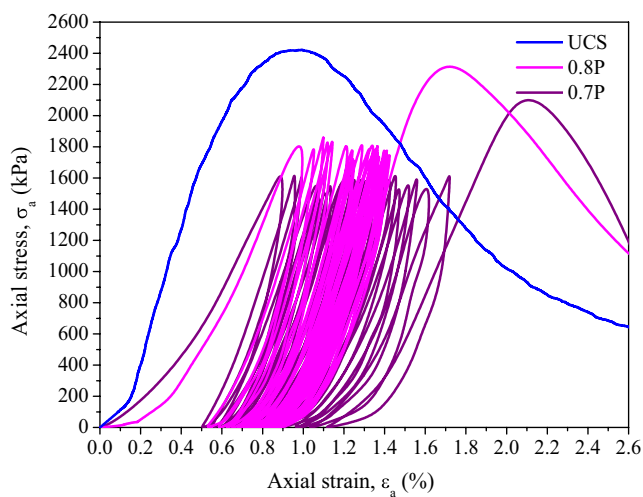
Fig. 13 Effect of activator ratio and 2 days thermal curing on cumulative mass loss, UCS and indirect tensile strength

The decrease in the strength was mainly attributed to lower alkalinity levels (due to low NaOH content) and the increase of silica content decreased the rate of strength gain [55]. No degradation in UCS and indirect tensile strength were observed on cyclic exposure to freezing and thawing for specimens with an activator ratio of 1:1. On the other hand, a reduction in UCS and indirect tensile strength of about 21.25% and 37.53%, respectively were noticed for specimens with an activator ratio of 1:2.5 on cyclic exposure to freezing and thawing. Further, an UCS value of about 2050 kPa was attained for thermal cured (60 °C) specimens, while an UCS of 2400 kPa was observed for ambient cured (25 °C) specimens. Moreover, an increase in UCS and indirect tensile strength of about 46.86% and 13.22%, respectively

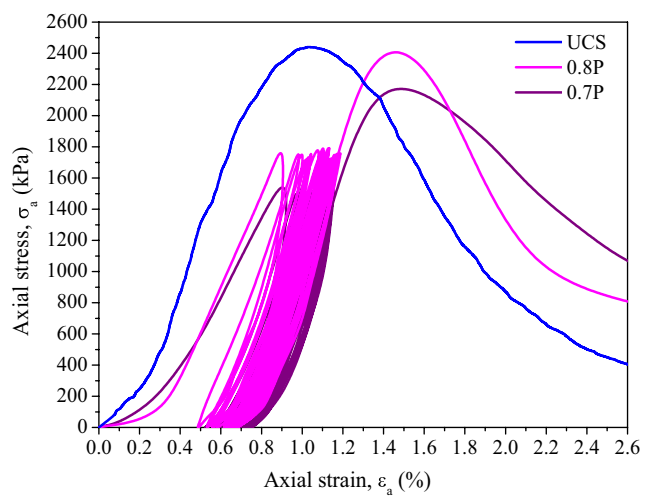
were observed in thermal cured specimens on exposure to freezing and thawing. The increase in the UCS and indirect tensile strength may be attributed to possible reinitiation of hydration reactions during the thawing phase with the availability of unreacted GGBS and activator in the presence of water.

Performance of Stabilized LMSF under Cyclic Loading Conditions

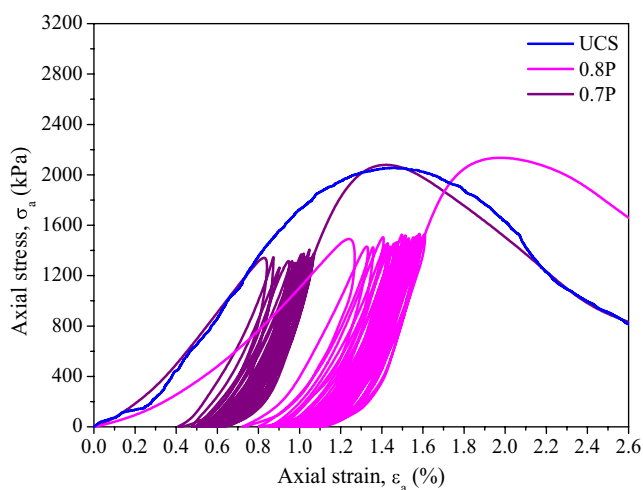
Cyclic UCS tests were conducted on combinations satisfying the minimum 28 days cured UCS requirements of sub-base and base course applications (2000 kPa as per AUSTRROADS [43]). The combinations with ambient curing



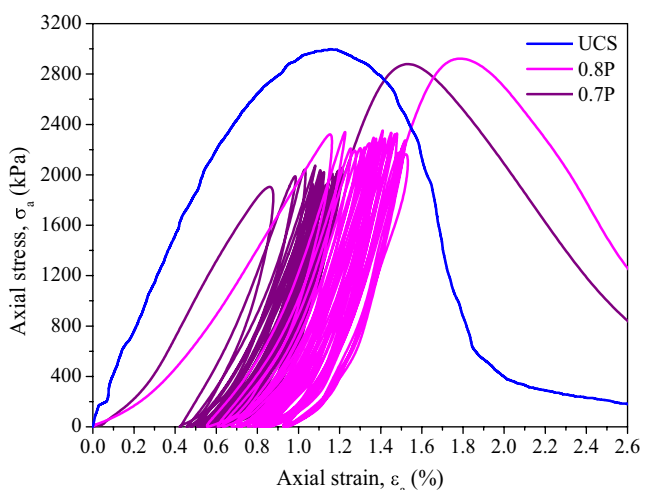
(a) Ambient curing without exposure to freeze-thaw cycles



(b) Ambient curing with exposure to freeze-thaw cycles



(c) Thermal curing without exposure to freeze-thaw cycles



(d) Thermal curing with exposure to freeze-thaw cycles

Fig. 14 Cyclic UCS test results for ambient and 2 days thermal cured specimens with and without exposure to freeze-thawing cycles

(25 °C for 56 days) and thermal curing (2 days at 60 °C followed by 53 days at – 21 °C and 1 day rest period at 25 °C) with and without cyclic exposure (at – 21 °C) in closed system were selected for cyclic UCS tests. Two different load intensities of 0.7P and 0.8P (where P is the respective peak UCS strength) were considered for cyclic loading, and the specimens were subjected to loading until failure, after 25 cycles. Figure 14 presents the axial stress versus strain response obtained from cyclic loading tests. When specimen was loaded until failure after 25 cycles, a reduction in the peak stress of about 6.10–14.30%, as compared to UCS value, was observed in ambient cured conditions (without exposure); wherein, negligible reduction of peak stress was observed for thermal cured specimens (without exposure), at 0.8P and 0.7P loading conditions as shown in Fig. 14a, c respectively. Similar response was observed in specimens exposed to freezing and thawing cycles as well. A reduction in peak stress in the range of 2.04% to 10.20% was observed in ambient cured specimens, as compared to UCS value; and negligible degradation was noticed in thermal cured specimens even after exposure to freezing and thawing cycles as shown in Fig. 14b, d. The present findings suggest that specimens subjected to 2 days of initial thermal curing, exhibit superior performance under cyclic loading conditions, indicating better strength and durability characteristics.

Challenges, Applications and Future Research Prospects on Utilization of LMSF

Several challenges such as possible presence of organic matter and heavy metals, wide variability in engineering behaviour, heterogeneity in composition, etc. could potentially limit the utilization of LMSF as alternate material. Detailed characterization of LMSF is essential to understand its properties and its heterogeneity in composition. Further, pre-processing of the LMSF obtained from landfill site to remove any residual undesired fraction is recommended to improve the viability of LMSF for various applications. Furthermore, by adopting suitable pre-treatment and stabilization methods, the challenges associated with LMSF can be addressed, which could potentially enhance the utilization of LMSF for various infrastructure applications. Pre-treatment technologies such as soil washing, soil vitrification and/or bioremediation can be useful for remediation/reduction in the heavy metal concentration. By adopting suitable stabilization method, the overall engineering behaviour of the LMSF can be enhanced to meet the target requirements. Treated LMSF can potentially serve as an alternate material for different infrastructure applications such as general backfill and structural fill material, stabilized subbase or base layer, and as fill material for embankments.

In the current study, alkali activated stabilization method was adopted to stabilize LMSF for its potential utilization in infrastructure applications under different climatic conditions. The study findings revealed stable and efficient performance of stabilized LMSF in different climatic conditions ranging from sub-freezing to arid conditions, when prolonged exposure to water was not expected. However, sub-freezing temperatures (below 0 °C), accompanied by high-water table and heavy rainfall (where percolation of water in LMSF pores was expected) conditions, may require further protective barriers or coatings to prevent erosion of unreacted particles from stabilized LMSF matrix. Initial thermal curing at 60 °C could benefit in improving the performance of stabilized LMSF in such conditions, as noted in the present study. Overall, the stabilized LMSF has shown potential as an alternate material source under different climatic conditions, with suitable curing/protection measures in sub-freezing temperatures. Further studies on evaluating the long-term performance of stabilized LMSF would be quite useful in advancing the understanding of its behaviour.

Conclusions

The study investigated the utilization of Landfill mined soil-like fraction (LMSF) as an alternative material to natural soils, employing alkali activated slag stabilization. The performance of stabilized LMSF was evaluated on exposure to different climatic conditions. The following conclusions were derived from the study:

- An optimum binder content of 40% with an activator content of 6% yielded better results in terms of unconfined compressive strength. A reduction in the UCS was observed with the increase of NaOH:Na₂SiO₃ ratio from 1:1 to 1:2.5 due to low alkalinity levels.
- Initial thermal curing at 60 °C for 2 days followed by 5 days curing at – 21 °C yielded a maximum UCS of about 2900 kPa within 7 days, attributed to reduced dilution of activator and higher pH levels, while ambient cured (25 °C) specimens yielded an UCS of 1750 kPa with 7 days of curing.
- A maximum mass loss of 18.49% was observed, when stabilized LMSF specimens were exposed to 12 cycles of freezing (– 21 °C) and thawing (25 °C) in open system, attributed mainly due to wetting induced erosion and spalling of surface due to freezing of pore water. However, for all the other exposure conditions, the degradation of specimens was limited and satisfied the minimum requirements of 14% as per IRC-37.
- Reduction in UCS values of about 25% and 60% was observed for the specimens exposed to 12 cycles of freezing/sub-freezing temperatures (0 °C and – 21 °C), respec-

tively, in open system; while, no noticeable reduction in UCS values was observed for other exposure conditions (10 °C, 25 °C and 45 °C) in open system (water inundated) and for all exposure conditions in closed system (no exposure to water). An increase in indirect tensile strength of about 16–25% was observed for specimens exposed to different climatic conditions in open system as compared to closed system, wherein no significant change was noticed.

- The microstructural aspects (based on FTIR spectra and optical imaging) revealed the stability of cementitious compounds on exposure to different climatic conditions. Though some disintegration and micro cracking were observed in open system, especially under sub-freezing conditions, a much homogeneous cementation was observed in the specimens due to the possible leaching of the activator solution into the LMSF pores.
- Thermal curing at 60 °C for 2 days followed by further curing at – 21 °C for 26 days yielded lower mass loss, and minimal reduction in UCS and tensile strength compared to ambient curing at 25 °C for 28 days. Additionally, cyclic loading at 80% and 70% of peak static failure load (UCS value) yielded negligible reduction in peak failure load after 25 cycles for 2 days thermal cured specimens, indicating higher resistance to fatigue effects. Hence, the study recommends initial thermal curing (at 60 °C) to enhance the strength and durability of alkali activated slag stabilized LMSF for various infrastructure applications, especially for cold regions.
- Overall, the findings of the study support the potential of stabilized LMSF as an alternative material resource in different climatic conditions for various infrastructure applications, including general backfill, structural fill, pavement subbase and base courses, and fill material for embankments. Further, the study makes a small step forward towards achieving United Nations sustainability development goals in the areas of sustainable infrastructure development and waste management.

Acknowledgement The authors are thankful to their institute, IIT-RAM for providing support and required facilities for conducting the research work. The authors are also thankful to Dr. Mahesh Mungule for support in FTIR analysis and sharing his insights related to alkali activation processes. Thanks, are also extended to Ms. Parish Dalal for performing the FTIR tests on the samples in the study. The authors also acknowledge the FTIR studies (ATR-IR) conducted at IITRAM, Courtesy: SERB-DST project ECR/2016/001289 sponsored FT-IR spectrometer (Make: PerkinElmer, USA). The authors express thanks to Central Instrumentation Facility, IIT Gandhinagar for facilitating the XRD and ICP analysis of samples. The authors also express thanks to Sophisticated Analytical Instrument Facility (SAIF), IIT Bombay for facilitating the ESEM/SEM and TGA analysis of samples. Thanks, are also extended to Ahmedabad Municipal Corporation for facilitating the procurement of landfill mined soil-like fraction (LMSF) for the present study.

Data Availability The data can be made available on reasonable request to the corresponding author.

Declarations

Conflict of Interest The authors have no relevant financial or non-financial interests to disclose.

References

1. Somani M, Datta M, Ramana GV, Sreekrishnan TR (2018) Investigations on fine fraction of aged municipal solid waste recovered through landfill mining: case study of three dumpsites from India. *Waste Manage Resea* 36(8):744–755. <https://doi.org/10.1177/0734242X18782393>
2. Chandana N, Goli VSNS, Mohammad A, Singh DN (2021) Characterization and utilization of landfill-mined-soil-like-fractions (LFMSF) for sustainable development: a critical appraisal. *Waste Biomass Valoriz* 12(2):641–662. <https://doi.org/10.1007/s12649-020-01052-y>
3. Song YS, Yun JM, Hong WP, Kim TH (2003) Investigation of solid waste soil as road construction material. *Environ Geol* 44(2):203–209. <https://doi.org/10.1007/s00254-002-0746-1>
4. Rawat P, Mohanty S (2021) Experimental investigation on MSW fine mixed with fibers: fiber reinforced waste. *J Hazard Toxic Radioact Waste* 25(3):04021009. [https://doi.org/10.1061/\(asce\)hz.2153-5515.0000609](https://doi.org/10.1061/(asce)hz.2153-5515.0000609)
5. Reddy AS, Wanare R, Rotte VM, Iyer KKR, Dave TN (2024) Performance of fibre-reinforced landfill mined soil like fraction as an environment friendly fill material. *J Environ Manage* 349:119464. <https://doi.org/10.1016/j.jenvman.2023.119464>
6. Reddy AS, Mungule M, Dave TN, Iyer KKR (2023) Evaluation of interface behaviour and load-settlement characteristics of geosynthetics-reinforced landfill mined soil like fraction for fill applications. *Int J Geosynth Ground Eng* 9(6):1–22. <https://doi.org/10.1007/s40891-023-00501-7>
7. Rawat P, Mohanty S (2024) Static and dynamic loading effects on the strength characteristic of municipal solid waste (MSW) fines reinforced with geosynthetics. *Sādhana* 49(1):7. <https://doi.org/10.1007/s12046-023-02359-x>
8. Ram AK, Rawat P, Mohanty S (2023) Strength performance of soil-fly ash-MSW fine layered system under different controlled loading conditions: a comparative study. *Constr Build Mater* 369:130524. <https://doi.org/10.1016/j.conbuildmat.2023.130524>
9. Wang D, Wang R, Benzerzour M, Wang H, Abriak NE (2020) Comparison between reactive MgO- and Na₂SO₄-activated low-calcium fly ash-solidified soils dredged from East Lake, China. *Marine Geotechnol* 38(9):1046–1055. <https://doi.org/10.1080/1064119X.2019.1648616>
10. Abdila SR, Abdullah MMAB, Ahmad R, Rahim SZA, Rychta M, Wnuk I, Nabialek M, Muskalski K, Tahir MFM, Syafwandi IM, Guwca M (2021) Evaluation on the mechanical properties of ground granulated blast slag (GGBS) and fly ash stabilized soil via geopolymer process. *Materials* 14(11):1–19. <https://doi.org/10.3390/ma14112833>
11. Reddy AS, Iyer KKR, Dave TN (2024) Alkali activated soil stabilization as a sustainable pathway for the development of resilient geotechnical infrastructure. *Indian Geotech J.* <https://doi.org/10.1007/s40098-024-00893-x>
12. Aldaood A, Bouasker M, Al-Mukhtar M (2014) Impact of freeze-thaw cycles on mechanical behaviour of lime stabilized gypseous soils. *Cold Reg Sci Technol* 99:38–45. <https://doi.org/10.1016/j.coldregions.2013.12.003>

13. Badakhshan E, Noorzad A, Vaunat J (2023) Stabilization of soft clays exposed to freeze–thaw cycles using chitosan. *J Cold Reg Eng* 37(2):04023004. <https://doi.org/10.1061/JCRGEL.CRENG-690>
14. Altun S, Sezer A, Erol A (2009) The effects of additives and curing conditions on the mechanical behaviour of a silty soil. *Cold Reg Sci Technol* 56(2–3):135–140. <https://doi.org/10.1016/j.coldregions.2008.11.007>
15. Jafari M, Esna-ashari M (2012) Effect of waste tire cord reinforcement on unconfined compressive strength of lime stabilized clayey soil under freeze–thaw condition. *Cold Reg Sci Technol* 82:21–29. <https://doi.org/10.1016/j.coldregions.2012.05.012>
16. Ajmera B, Emami AH (2024) Review of the impact of permafrost thawing on the strength of soils. *J Cold Reg Eng* 38(2):03124001. <https://doi.org/10.1061/JCRGEL.CRENG-727>
17. Zhu X, Niu F, Ren L (2023) Novel selection of environment-friendly curing agents for thawing permafrost: alkali-activated ground granulated blast-furnace slag. *Cold Reg Sci Technol* 211:103863. <https://doi.org/10.1016/j.coldregions.2023.103863>
18. Bai L, Yang Z, Wu Y, Anbarlouie M, Pan Z (2023) Stabilization of aeolian sand for pavement subbase applications using alkali-activated fly ash and slag. *Minerals* 13(3):453. <https://doi.org/10.3390/min13030453>
19. Aryal S, Kolay PK (2020) Long-term durability of ordinary Portland cement and polypropylene fibre stabilized kaolin soil using wetting–drying and freezing–thawing test. *Int J Geosynth and Ground Eng* 6:1–15. <https://doi.org/10.1007/s40891-020-0191-9>
20. Fakhrabadi A, Choobasti AJ, Kutanaei SS (2023) Durability evaluation of clayey sandy soil stabilized with copper-slag-based geopolymer under freezing–thawing cycles. *Int J Pavem Res Technol*. <https://doi.org/10.1007/s42947-023-00341-8>
21. Jamalimoghadam M, Bahmyari H (2023) Freeze–thaw characteristics of slaking marl clay stabilized with a binder based on alkali-activated recycled glass powder. *J Mater Civ Eng* 35(11):04023394. <https://doi.org/10.1061/JMCEE7.MTENG-15432>
22. Samantasinghar S, Singh SP (2021) Strength and durability of granular soil stabilized with FA-GGBS geopolymer. *J Mater Civ Eng* 33(6):06021003. [https://doi.org/10.1061/\(ASCE\)MT.1943-5533.0003736](https://doi.org/10.1061/(ASCE)MT.1943-5533.0003736)
23. ASTM D2487 (2018) Standard practice for classification of soils for engineering purposes (unified soil classification system)
24. ASTM D4318 (2018) Standard test methods for liquid limit, plastic limit and plasticity index of soils
25. ASTM D2974 (2020) Standard test methods for determining the water (moisture) content, ash content, and organic material of peat and other organic soils
26. ASTM D854-14 (2014) Standard test methods for specific gravity of soil solids by water pycnometer. ASTM international, Conshohocken
27. ASTM D698-12 (2021) Test methods for laboratory compaction characteristics of soil using standard effort (12 400 ft-lbf/ft³ (600 kN m/m³))
28. ASTM D2166 (2016) Standard test method for unconfined compressive strength of cohesive soil
29. ASTM D3987 (2020) Standard practice for shake extraction of solid waste with water
30. Walker JM (1996) U.S. environmental protection agency regulations for compost production and use. *The Sci Compost*. https://doi.org/10.1007/978-94-009-1569-5_34
31. VLAREBO (2008) Vlaams regelment bodemsanering flemish soil remediation decree
32. Sanchora P, Pandey DK, Rana D, Materny A, Singh DK (2019) Impact of size and electronegativity of halide anions on hydrogen bonds and properties of 1-ethyl-3-methylimidazolium-based ionic liquids. *J Phys Chem A* 123(23):4948–4963. <https://doi.org/10.1021/acs.jpca.9b04116>
33. Maragkos I, Giannopoulou IP, Panias D (2009) Synthesis of feronickel slag-based geopolymers. *Miner Eng* 22(2):196–203. <https://doi.org/10.1016/j.mineng.2008.07.003>
34. Zaharaki D, Komnitsas K, Perdikatsis V (2010) Use of analytical techniques for identification of inorganic polymer gel composition. *J Mater Sci* 45:2715–2724. <https://doi.org/10.1007/s10853-010-4257-2>
35. Xu B (2021) Utilization of ladle slag for soil stabilization. Nanyang Technological University. <https://hdl.handle.net/10356/152773>
36. Aydin S, Baradan B (2014) Effect of activator type and content on properties of alkali-activated slag mortars. *Compos Part B Eng* 57:166–172. <https://doi.org/10.1016/j.compositesb.2013.10.001>
37. ASTM C496 (2017) Standard test method for splitting tensile strength of cylindrical concrete specimens
38. ASTM D560 (2012) Standard test methods for freezing and thawing compacted soil–cement mixtures
39. Wong LC, Haug MD (1991) Cyclical closed-system freeze–thaw permeability testing of soil liner and cover materials. *Can Geotech J* 28(6):784–793. <https://doi.org/10.1139/t91-095>
40. Jones CW (1987) Long term changes in the properties of soil linings for canal seepage control (Report No. REC-ERC-87-1). U.S. Department of the Interior, Bureau of Reclamation, Engineering and Research Center, Denver
41. Feng S, Ibrahim E, Vardanega PJ (2023) Hydraulic conductivity of fine-grained soils subjected to freeze–thaw cycles. *Cold Reg Sci Technol* 213:103902. <https://doi.org/10.1016/j.coldregions.2023.103902>
42. Güllü H, Khudir A (2014) Effect of freeze–thaw cycles on unconfined compressive strength of fine-grained soil treated with jute fiber, steel fiber and lime. *Cold Reg Sci and Technol* 106:55–65. <https://doi.org/10.1016/j.coldregions.2014.06.008>
43. AUSTRROADS (2008) Guide to pavement technology part 2: pavement structural design, AGPT02-08
44. Horgnies M, Chen JJ, Bouillon C (2013) Overview about the use of Fourier transform infrared spectroscopy to study cementitious materials. *WIT Trans Eng Sci* 77:251–262
45. Fernandez L, Alonso C, Hidalgo A, Andrade C (2005) The role of magnesium during the hydration of C3S and CSH formation. *Scanning electron microscopy and mid-infrared studies*. *Adv Cem Res* 17(1):9–21. <https://doi.org/10.1680/adcr.2005.17.1.9>
46. Xu H, Van Deventer JSJ (2003) The effect of alkali metals on the formation of geopolymeric gels from alkali-feldspars. *Coll Surf A Physicochem Eng Aspects* 216(1–3):27–44. [https://doi.org/10.1016/S0927-7757\(02\)00499-5](https://doi.org/10.1016/S0927-7757(02)00499-5)
47. Miraki H, Shariatmadari N, Ghadir P, Jahandari S, Tao Z, Siddique R (2022) Clayey soil stabilization using alkali-activated volcanic ash and slag. *J Rock Mech Geotech Eng* 14(2):576–591. <https://doi.org/10.1016/j.jrmge.2021.08.012>
48. Pourakbar S, Huat BBK, Asadi A, Fasihnikoutalab MH (2016) Model study of alkali-activated waste binder for soil stabilization. *Int J Geosynth Ground Eng* 2:1–12. <https://doi.org/10.1007/s40891-016-0075-1>
49. Provis JL, Palomo A, Shi C (2015) Advances in understanding alkali-activated materials. *Cem Conc Res* 78:110–125. <https://doi.org/10.1016/j.cemconres.2015.04.013>
50. Abdeldjoud L, Asadi A, Nahazanan H, Huat BB, Dheyab W, Elkhebu AG (2019) Effect of clay content on soil stabilization with alkaline activation. *Int J Geosynth Ground Eng* 5:1–8. <https://doi.org/10.1007/s40891-019-0157-y>
51. IRC-37 (2018) Guidelines for the design of flexible pavements. New Delhi, India
52. Orakoglu ME, Liu J, Lin R, Tian Y (2017) Performance of clay soil reinforced with fly ash and lignin fiber subjected to

- freeze-thaw cycles. *J Cold Reg Eng* 31(4):04017013. [https://doi.org/10.1061/\(ASCE\)CR.1943-5495.0000139](https://doi.org/10.1061/(ASCE)CR.1943-5495.0000139)
53. Syed M, GuhaRay A, Goel D, Asati K, Peng L (2020) Effect of freeze–thaw cycles on black cotton soil reinforced with coir and hemp fibres in alkali-activated binder. *Int. J Geosynth Ground Eng* 6:1–15. <https://doi.org/10.1007/s40891-020-00200-7>
54. Wu Y, Lu B, Bai T, Wang H, Du F, Zhang Y, Cai L, Jiang C, Wang W (2019) Geopolymer, green alkali activated cementitious material: synthesis, applications and challenges. *Constr Build Mater* 224:930–949. <https://doi.org/10.1016/j.conbuildmat.2019.07.112>
55. Singh A, Bhadauria SS, Thakare AA, Kumar A, Mudgal M, Chaudhary S (2024) Durability assessment of mechanochemically activated geopolymer concrete with a low molarity alkali solution.

Case Stud Construct Mater 20:e02715. <https://doi.org/10.1016/j.cscm.2023.e02715>

Publisher's Note Springer Nature remains neutral with regard to jurisdictional claims in published maps and institutional affiliations.

Springer Nature or its licensor (e.g. a society or other partner) holds exclusive rights to this article under a publishing agreement with the author(s) or other rightsholder(s); author self-archiving of the accepted manuscript version of this article is solely governed by the terms of such publishing agreement and applicable law.